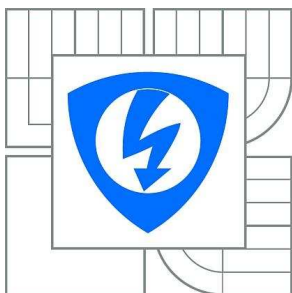


VYSOKÉ UČENÍ TECHNICKÉ V BRNĚ

BRNO UNIVERSITY OF TECHNOLOGY



FAKULTA ELEKTROTECHNIKY A KOMUNIKAČNÍCH
TECHNOLOGIÍ

ÚSTAV ELEKTROTECHNOLOGIE

FACULTY OF ELECTRICAL ENGINEERING AND COMMUNICATION
DEPARTMENT OF ELECTRICAL AND ELECTRONIC
TECHNOLOGY

SIMULACE I-U CHARAKTERISTIK FOTOVOLTAICKÝCH MODULŮ

SIMULATION OF I-V CHARACTERISTIC ON PHOTOVOLTAIC MODULES

DIPLOMOVÁ PRÁCE

MASTER'S THESIS

AUTOR PRÁCE

AUTHOR

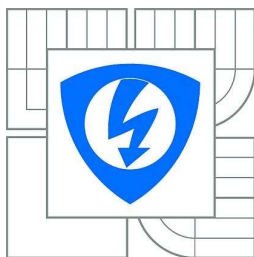
Bc. JAN JIŘÍK

VEDOUCÍ PRÁCE

SUPERVISOR

Ing. PETR KŘIVÍK, Ph.D.

BRNO 2010



VYSOKÉ UČENÍ
TECHNICKÉ V BRNĚ

Fakulta elektrotechniky
a komunikačních technologií

Ústav elektrotechnologie

Diplomová práce

magisterský navazující studijní obor
Elektrotechnická výroba a management

Student: Bc. Jan Jiřík

ID: 83686

Ročník: 2

Akademický rok: 2009/2010

NÁZEV TÉMATU:

Simulace I-U charakteristik fotovoltaičských modulů

POKYNY PRO VYPRACOVÁNÍ:

Seznamte se s I-U a P-U charakteristikami fotovoltaičských modulů a s možnostmi jejich simulace.

Osvojte si základy práce s programem VEE Pro 8.0.

Vytvořte program simulující I-U a P-U charakteristiky fotovoltaičského modulu.

Výsledné charakteristiky získané programem porovnejte s charakteristikami naměřenými na reálném fotovoltaičském modulu.

DOPORUČENÁ LITERATURA:

In conformity with the instructions of the Head of thesis.

Termín zadání: 8.2.2010

Termín odevzdání: 15.8.2010

Vedoucí práce: Ing. Petr Křivík, Ph.D.

prof. Ing. Jiří Kazelle, CSc.

Předseda oborové rady

UPOZORNĚNÍ:

Autor diplomové práce nesmí při vytváření diplomové práce porušit autorská práva třetích osob, zejména nesmí zasahovat nedovoleným způsobem do cizích autorských práv osobnostních a musí si být plně vědom následků porušení ustanovení § 11 a následujících autorského zákona č. 121/2000 Sb., včetně možných trestněprávních důsledků vyplývajících z ustanovení části druhé, hlavy VI. díl 4 Trestního zákoníku č.40/2009 Sb.

Abstract:

This thesis deals with the solar radiation, which is one of the potential sources of renewable energy. One of the main objectives is to let know about the problematic of the photovoltaic. Semi-automated measuring workplace is constructed, which gave us real I-V and P-V characteristic. The next main objective is to construct the program, which simulates these characteristic in the program Vee Pro 8.0. The goal is to obtain real characteristic constant for the real solar panel.

Abstrakt:

Tato práce se zabývá slunečním zářením, které je jedním z možných zdrojů obnovitelné energie. Hlavními body práce je seznámit se s problematikou fotovoltaiiky. Sestrojení poloautomatizovaného měřícího pracoviště, díky němuž obdržíme reálné I-U a P-U charakteristiky solárního panelu. Dalším bodem je sestrojení programu v programu Vee Pro 8.0, který tyto charakteristiky simuluje v programu. Cílem je zjistit charakteristické konstanty pro daný solární panel.

Keywords:

Photovoltaic, solar panel, simulation, I-V characteristic

Klíčová slova:

Fotovoltaiika, solární panel, simulace, I-U charakteristika

Bibliografická citace díla:

JIŘÍK, J. *Simulace I-U charakteristik fotovoltaiických modulů*. Brno: Vysoké učení technické v Brně, Fakulta elektrotechniky a komunikačních technologií, 2010. 57 s. Vedoucí diplomové práce Ing. Petr Křivík, Ph.D.

Prohlášení autora o původnosti díla:

Prohlašuji, že jsem tuto vysokoškolskou kvalifikační práci vypracoval samostatně pod vedením vedoucího diplomové práce, s použitím odborné literatury a dalších informačních zdrojů, které jsou všechny citovány v práci a uvedeny v seznamu literatury. Jako autor uvedené diplomové práce dále prohlašuji, že v souvislosti s vytvořením této diplomové práce jsem neporušil autorská práva třetích osob, zejména jsem nezasáhl nedovoleným způsobem do cizích autorských práv osobnostních a jsem si plně vědom následků porušení ustanovení § 11 a následujících autorského zákona č. 121/2000 Sb., včetně možných trestněprávních důsledků vyplývajících z ustanovení § 152 trestního zákona č. 140/1961 Sb.

Ve Valencii dne 1. 7. 2010

.....

Poděkování:

Děkuji vedoucímu diplomové práce Ing. Petru Křivíkovi, Ph.D. za účinnou metodickou, pedagogickou a odbornou pomoc a další cenné rady při zpracování diplomové práce.

I would like to say thanks to my professor Esteban Sanchis Ph.D. for his useful advice, methodic and pedagogic help and useful tips to write this diploma thesis.

CONTENT

CONTENT	5
1 INTRODUCTION	6
2 PHOTOVOLTAIC SOLAR PANEL	7
3 PHYSICAL PRINCIPLE.....	8
3.1 BAND THEORY OF SEMICONDUCTORS	8
3.2 SEMICONDUCTOR	10
3.3 P-N JUNCTION	13
3.4 FUNCTION OF SOLAR CELLS	15
4 PRODUCTION OF SOLAR CELLS.....	16
5 SIMULATION OF SOLAR CELL.....	19
5.1 DEPENDENCE OF TEMPERATURE ON THE WIDTH OF THE BAND GAP.....	19
5.2 SOLAR CELL FROM AN ELECTRONIC PERSPECTIVE	20
5.3 PARAMETERS OF SOLAR CELL AT LIGHT.....	23
5.4 INFLUENCE OF TEMPERATURE	26
5.5 SERIES AND PARALLEL CONNECTIONS OF SOLAR CELLS.....	28
6 SIMULATION	31
6.1 THE PROGRAMMING ENVIRONMENT	31
6.2 ABOUT.....	31
6.3 GRAPHIC DESIGN	32
6.4 PROGRAMMATIC DESIGN	32
6.5 EXAMPLE (INCREMENTAL METHOD).....	37
6.6 TEMPERATURE AND IRRADIANCE.....	40
7 MEASUREMENT OF I-V CHARAKTERISTIC OF SOLAR PANEL.....	43
7.1 SOLAR PANEL WITH CIRCLE CELLS.....	45
7.2 SOLAR PANEL WITH RECTANGULAR CELLS	47
8 SEARCHING CONSTANTS OF SOLAR PANEL	49
8.1 SEARCHED CONSTANTS FOR SOLAR PANEL WITH CIRCLE CELLS.....	52
8.2 SEARCHED CONSTANTS FOR SOLAR PANEL WITH RECTANGULAR CELLS	53
9 CONLUSION AND OUTLOOK.....	55
LIST OF FIGURES	56
REFERENCES.....	57

1 INTRODUCTION

In this thesis, many aspects are based on photovoltaic. This is a "fundamental building block" of solar cells. From an empirical perspective, the word photovoltaic is formed by joining two different words. Photo comes from the Greek word photos. Volt comes from the name of the Italian physicist Alessandro Volta. Photovoltaic is the direct conversion of sunlight energy into electrical energy. In this area, research is carried out in different countries such as USA, throughout the EU, Japan, and many others scientific teams from around the world. Energy consumption is constantly rising, so it is very important for this research to be carried out. Thus, in terms of trends, the importance of photovoltaic as an energy source is constantly increasing, because it is inexhaustible and an environmentally friendly source of energy.

2 PHOTOVOLTAIC SOLAR PANEL

Solar cell allows direct conversion of solar energy into electricity. (solar cell is a large-sized semiconductor element with at least one P-N junction). In solar cells, there are excited electrically charged particles, for that reason electrons are separated by the internal electric field by P-N junction. The distribution of electric charge results in a voltage difference between the front (-) and rear (+) contact of the cell. DC current flows through load resistance, which is connected between the two contacts. DC current is proportional to the area of the solar cell and the intensity of incident light. A solar panel is produced after encapsulating and electrically connecting of solar cells. See Fig. 2.1.



Fig. 2.1: Solar panel

Energy conversion efficiency of solar irradiation into electrical energy, in currently produced solar cells, is up to 17%. Under laboratory conditions, the efficiency reaches up to 28%. A monocrystalline cell with area of $1 \cdot 10^{-2} \text{ m}^2$ is able to deliver to the load resistance current of 3A at a voltage of about 0.5V. At present, most solar cells are made from silicon crystal in the form of mono-crystal or multi-crystal. In production there are thin-film solar cells based on amorphous silicon. Already in production are applied the new CdTe thin-film technology, CIS and CIGS structures. [1], [2], [4]

3 PHYSICAL PRINCIPLE

3.1 Band theory of semiconductors

In general, solid is the place where photons are converted into electrical energy. Silicon is the most commonly used element in photovoltaic. Silicon is an elementary semiconductor of the group IV of the Mendeleev's periodic table of elements. Then as we already know, silicon has four valence electrons in the outer shell. In order to obtain the most stable electron configuration, neighbouring atoms in the silicon crystal lattice form an electron pair binding. In other words, two atoms both share and use these electrons. There emerge electron pair bindings (covalent bonds) with four neighbouring atoms. It gives silicon a stable electron configuration. In the energy band model, the valence band is now fully occupied and the conduction band is empty. Current can flow only when an electron gets from valence band to conduction band. Supplying sufficient energy by incident light or heat can elevate an electron from the valence band into the conduction band. This energy must overcome the band gap (Forbidden band), which lies between the conduction band and the valence band. See Fig. 3.1.

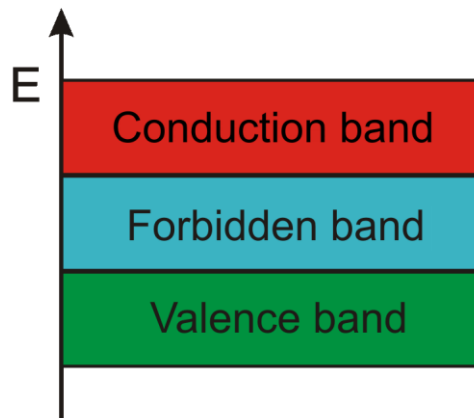


Fig. 3.1: Band model

Note: The size of the band gap depends on the physical properties of the material, and mainly depends on the grid constant. According to the size of the band gap, these substance are subdivided to conductors, semiconductors and isolators. The valence and conduction bands overlap in the case of conductors. In the case of isolators, the conduction band is empty, because the forbidden band is too big. Semiconductors have also band gap, but it is not so big and electrons can elevate to conduction band. However, due to the lower band gap ($E_g < 5$ eV), electrons can be lifted to the conduction band. Substances with a bigger band gap E_g then 5 eV are considered as isolators. In the case of semiconductors, electrons are tightly bounded

to their atoms actually corresponding to the occupied level in valence belt. In the energy band model, the valence band is now fully occupied and the conduction band is empty. If sufficient energy is supplied, the electron inside the crystal structure may be released from their atoms and be able to move freely. This energy can be thermal (phonon) or light (photon). This energy can elevate an electron from the valence band into the conduction band, thus enabling the electron to move easily through the crystal lattice. In the valence band, remains a defect electron or hole. The formation of defect electrons is responsible for the intrinsic conduction of semiconductors. In the silicon atom after influence of sufficient energy a hole is formed, because the electron went to another position (to the valence band). Once again in the hole can be trapped a free electron (the same or another). This is reflected in the energy bands scheme as a retransfer of electrons from conduction band to the corresponding level in the valence band. Another possibility is that, in the place of the electron hole, a leaping neighbouring atom can firmly bind. For this to happen, there needs to be enough energy to be able to overcome an energy barrier. This will move the hole to the neighbouring atom. This situation may be repeated several times and due to these jumps an electron hole can move further. Free and leaping bounded electrons in electric field move against the direction of its intensity, because they have a negative electrical charge. On the contrary, the holes move in the direction of electric field intensity and behave as particles with an electrical positive charge. They have greater materiality than a free electron.

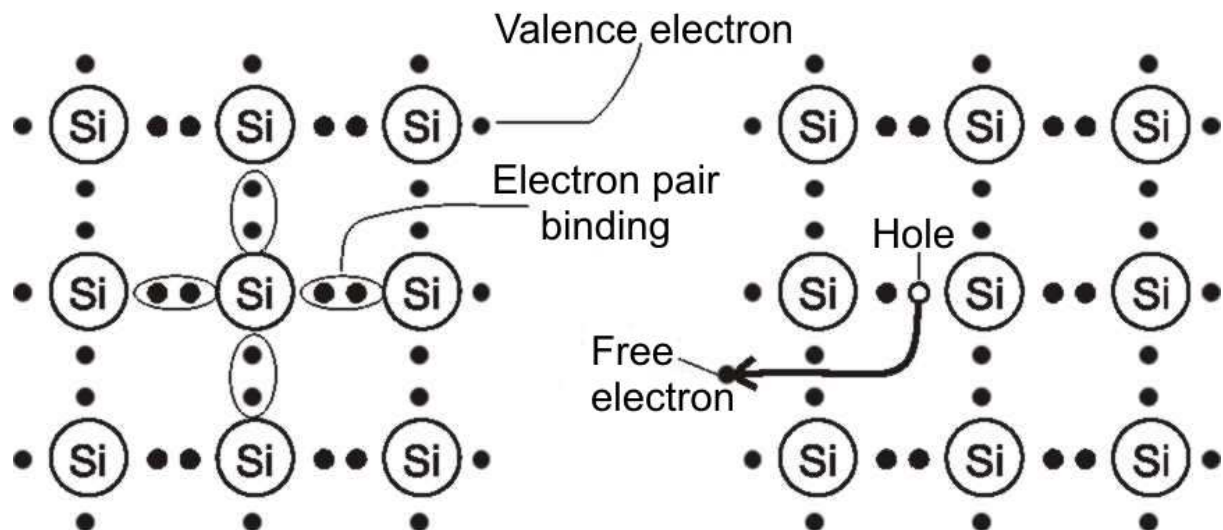


Fig. 3.2: Crystal Structure of Silicon (left), intrinsic conduction due to defect electron in the crystal lattice (right)

From chemical aspect, it is possible to join elements from another group as it is shown in the following picture Fig. 3.3. (Phosphorus is from group V, Boron is from group III). [2], [3], [6].

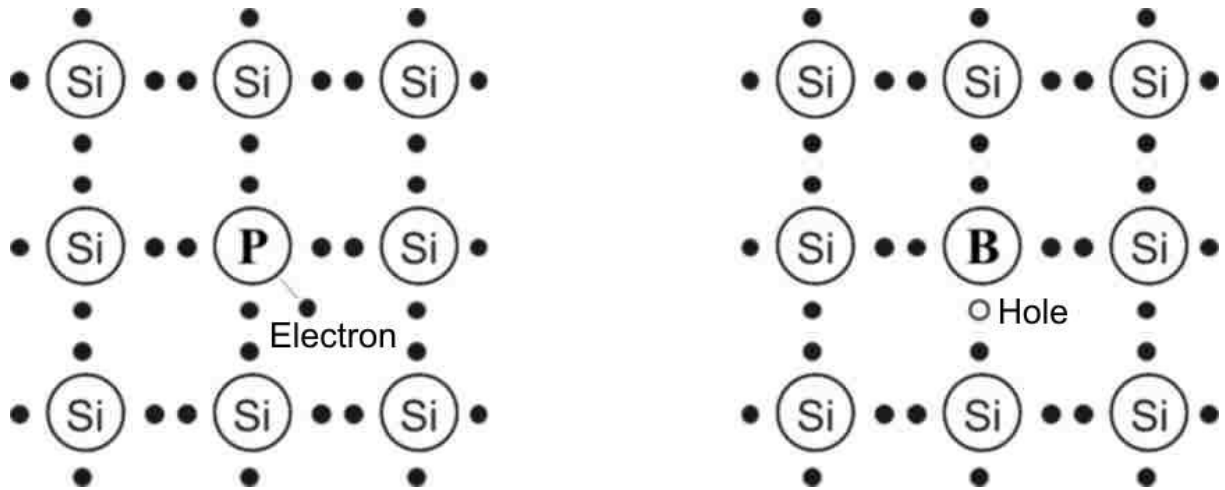


Fig. 3.3: Defect Conduction for n-type (left) and p-type doped silicon (right)

3.2 Semiconductor

As already indicated in the previous chapter, the release of one electron creates a hole. From outside view, the semiconductor seems like electrically neutral, because the number of free electrons is always equal to the number of holes. If the impact of a photon generates a pair of an electron - hole, then energy of photon will have to be greater or at least equal to the width of the band gap. Photons that have less energy pass through the semiconductor and those electrons with energy greater or equal to the width of the band gap are absorbed in the conduction band. The width of the band gap in silicon is ≈ 1.1 eV, so it is transparent to photons with lower energies, which corresponds to wavelengths larger than $\lambda \geq 1100$ nm, which can be determined from the following equation:

$$E = \frac{hc}{\lambda} \quad (1)$$

Where: h..... Planck constant

c..... Speed of light

λ Wavelength

In the following Fig. 3.4 it is possible to see the important characteristics of semiconductors. Case a) shows, function $g(E)$. This function represents the density of states, respectively shows a number of states per energy interval unit in valence band and

conductivity band, depending on energy. In another case, the same Fig. 3.4, however, case b) shows the so-called distribution function $f(E)$, which indicates the probability of occupancy of state with energy E by electron. Value $1 - f(E)$ is the probability of hole occupancy status. The probability that the electron will have the same energy as the Fermi level is 0.5. Fermi level is the imaginary centre of the band gap. The electrons are governed by Fermi-Dirac statistics, because they belong to a group of particles called fermions. This distribution function can be expressed by the following equation:

$$f(E) = \frac{1}{e^{\frac{E-E_F}{kT}} + 1} \quad (2)$$

Where: k Boltzmann constant

T The absolute thermodynamic temperature

In the last case, Fig. 3.4 part c) functions:

$f(E)g(E) = n(E)$ indicates the concentration of electrons in the conductivity band
 $1 - f(E) g(E) = p(E)$ indicates the concentration of holes in the valence band.

Note: The areas under curves 1 and 2 are proportional to these concentrations. In its intrinsic semiconductors, these areas are the same size.

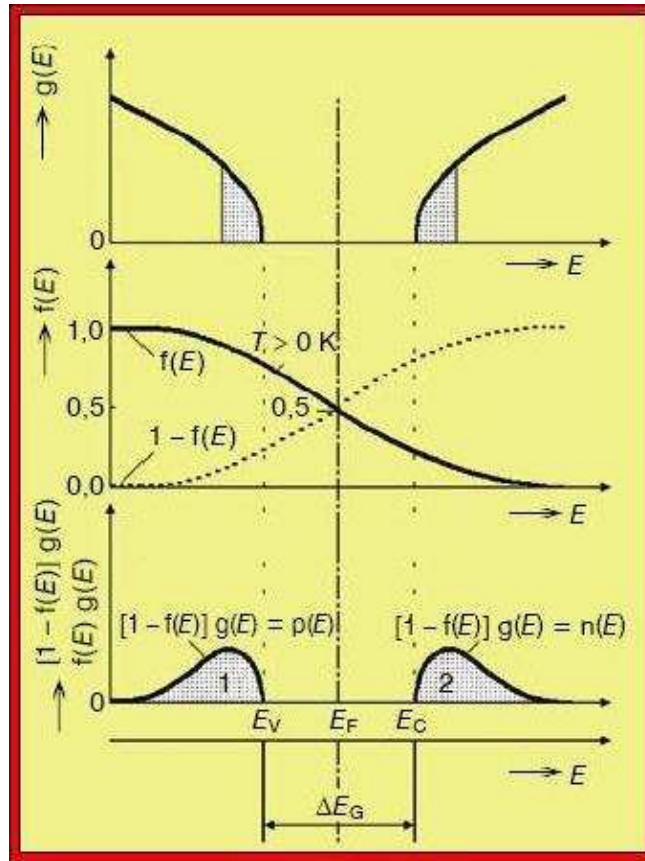


Fig. 3.4: Model of electrons and holes of intrinsic semiconductor

Note: N-type semiconductor silicon crystal forms, when silicon atom is replaced by some element from the V group of Mendeleev's table. Most often elements are As, P or Sb. If these atoms are embedded into a silicon crystal lattice, the fifth electron will not participate in the electron pair binding. Thus, this electron is not too much embedded in the structure and can easily lose this position. Little energy is required to separate this electron from the atom and thus create a free electron. The energy required to transfer electrons from the valence band into the conduction band is relatively low, approximately $\Delta E_D \approx 0.012$ eV. The electron can then easily move to the conduction band even at room temperature, that is the supply of heat energy $kT = 0.025$ eV. Fermi energy level is then moved towards higher energies. The embedding of atoms from group V is called N-doping. The “impurity atoms” are called donors.

In analogy to N-type semiconductors, P-type semiconductor silicon crystal forms, when silicon atom in the silicon crystal lattice is changed by the element from the III group of Mendeleev's table. Typical representatives are the elements Al, B or Ga. These elements have only three-bindings (they have only three valence electrons). This fact creates a missing valence electron and thus holes emerge as the majority carriers. This process is called

P-doping. It makes the semiconductor of P-type and the “impurity atoms” are called acceptors. A small amount of energy ΔE_A can release a freely moving hole. Electron from a neighbouring atom can jump to the hole, so the hole will then move in the crystal. From the outside view, the acceptor atom seems to be negatively charged, because it has one electron more. This creates a fixed negative charge. A hole, which arises in this valence band, moves freely inside the crystal. Concentration of holes in the P-type semiconductor is greater than the concentration of free electrons. Fermi energy level is then moved towards lower energies. [2], [6]

3.3 P-N junction

A special case of non-homogeneous distribution of defect conduction (impurities) is a P-N junction (see Fig. 3.5). P-N junction is created when that part of the semiconductor is doped as P-type semiconductor and in the same time, the neighbouring part is doped as N-type semiconductor. In the P-N junction the gradient of concentration of free carriers N flows in the direction of the junction, which is evident from Fig. 3.5 respectively from part a). The direction is the same as the direction of x , N_D is the concentration of donors, N_A is the concentration of acceptors. Some electrons are diffused from the N-region into the P-region, and holes from the P-region into the N-region. Tightly coupled bound charge of ionized impurities creates the area of charge (the N-type semiconductor has positive charge region, as can be seen in Fig. 3.5 part c). In that area an electric field is created and this counteracts another free carriers. This is the reason why diffusion cannot continue indefinitely. Fermi energy level must be constant everywhere throughout the crystal, and therefore in the area of the junction the band bends. An idealized situation is shown in Fig. 3.5 part b). P-N junction width is given by point x_p and x_n . V_D is the potential difference between the differently doped regions (so-called diffusion voltage). This described junction may satisfy a simple P-N semiconductor diode. The system is not in static equilibrium state, but it is in a state of dynamic equilibrium. In the case that $T > 0$ K, there is a constant recombination and there is generation of electrons and holes also. From Fig. 3.5 part b) it is possible to see, that currents flow through the P-N junction in both directions. Due to graphic simplicity, only the flow of electrons is illustrated. Currents made by holes behave similarly. In the N-type semiconductor, some of the electrons may have higher energy than the corresponding potential barrier diffusion voltage V_D . These electrons can move through the P-N junction to part of the P-type semiconductor, where they do not combine with free holes. This current is

called recombination current. Simultaneously, P-type semiconductor generates couples of free electrons and holes. In an electric field of the P-N junction, free electrons are accelerated towards the area of N-type semiconductor. This current is called diffusion or thermal. Without the application of external voltage, currents in both directions are the same, so externally they cannot be viewed. In the case, that semiconductor with P-N junction is connected to a closed external electric voltage, it will provoke an unbalance. In the case that positive charge is connected on the area of P-type semiconductor, there will be a change in curvature of the belts. Potential barrier V_D will be reduced about the value of ΔV and thus prevails the flow of electrons into the P-type area of semiconductor and holes will flow in the reverse direction. P-N junction is then oriented in the forward direction. If external voltage is connected with the opposite polarity, it will increase potential barrier V_D , thereby it will reduce the recombination current flow. It begins to dominate the diffusion current, which is due to the low (smaller) concentration of electrons in area of P-type semiconductor. P-N junction is then oriented in reverse direction. [2], [6]

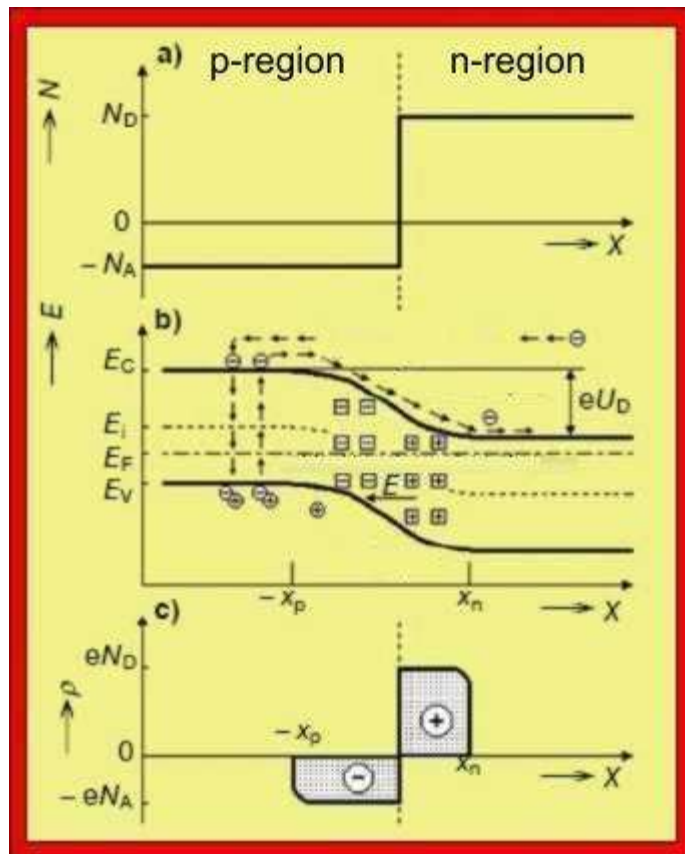


Fig. 3.5: Model of P-N junction

3.4 Function of solar cells

In Fig. 3.6 it is possible to see the cut of solar cells. As can be seen, on the front of the solar cell sunlight is illuminated (irradiance). This causes generation of positive and negative charges in the silicon crystal. Electric charges are separated in the semiconductor P-N junction. Electrons are in the N-type and positive charges are in the P-type of semiconductor. Material is always a large-scale-area semiconductor diode with one or more P-N junctions, regardless of the material. Currently manufactured cells do not exceed an area more than $2 \cdot 10^{-2} \text{ m}^2$ with a maximum thickness of $180 \text{ }\mu\text{m}$. Front solar cells are designed to do the smallest possible optical losses. Optical losses are caused by incomplete absorption and reflections of irradiation. Most of solar cells are designed so that they have front and rear contact. These contacts are used to connect wires. [2], [4], [6]

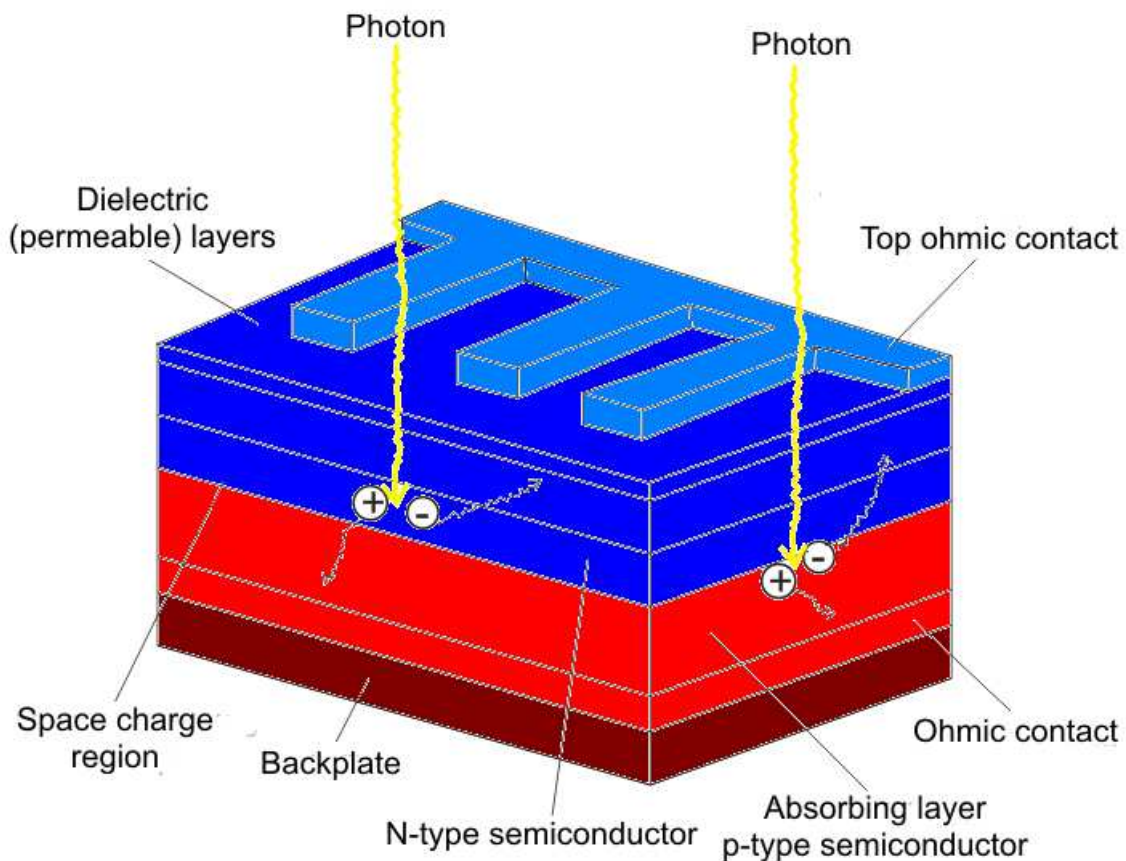


Fig. 3.6: Cut commonly produced typical solar cells

4 PRODUCTION OF SOLAR CELLS

In the manufacture of solar cells, there are several boundary-stones. There is a large influence of the financial factor on the development and production of technology. In the space program, the cost of producing solar cell is insignificant compared to transport costs, so in the space program the efficiency is much more important factor than the price. The opposite is the production of solar cells on Earth. On Earth, using the cheapest suitable material is the goal when producing solar cells. This is undoubtedly the silicon because of several reasons. It is available in unlimited quantities (about 1/3 of the Earth's crust is composed of silicon dioxide), so it is easily available and cheap, not toxic and does not adversely affect the environment. Successfully technology operations needed to create silicon structures were managed very well too. Silicon absorbs only the light with a wavelength of less than 1 μm . This corresponds to photons of energy greater than 1.1 eV. Therefore it can absorb the infrared spectrum, the whole visible and ultraviolet spectrum, so that a bigger part of the entire solar spectrum is absorbed.

In Fig. 4.2 it can be seen schematically, the process of manufacturing contacts by screen-printing and in Fig. 4.3 is a finished polycrystalline, square solar cell. Fig. 4.1 shows principally the process sequence illustrated schematically point by point:

The first working step is that rough slices of P-type semiconductor wet chemical boron subsidized are eaten-away by a few micrometers. This removes the crystal layer destroyed by cutting. It also clears slices.

This is followed by ordinary diffusion. In the electrically heated quartz tube at a temperature of + 800 °C phosphorus diffuses from the carrier gas to the surface layer of slices. This creates a layer with N-type doped and phosphorus highly enriched oxide layer.

After stacking the slices together, the slices are compressed into a compact cube and its edges, in the oxygen plasma produced by the action of high frequency, are eaten away. By this process N-type semiconductor layer is removed from the edges of the wafers.

The oxide layer is then removed from the front and backside by the wet chemical etching. Afterwards the contact from the conductive silver is stamped on the back area. This silver contains several percent of aluminium. This is done by screen-printing method which has been customary craft printing process for a long time. Serigraphy is well tight contexture from steel or plastic coated by photo-mask. Over this pattern is the conductive silver stamped on the wafers by spatula.

Following that is drying and a second printing, which prints only the contact area needed to consolidate the couplings between the solar cells.

Now both prints are high-temperature sintered. In doing so, there arises a large mechanical adhesion between the conductive paste and silicon wafer. At the same time, the aluminium contained in the conductive paste penetrates to the silicon slice, which changes the N-type region to the P-type region.

This is followed by printing a fingerprint-shaped contact on the front side, drying, printing anti-reflective coating, which causes bluish sheen of wafer, and eventually common sintering. [1]

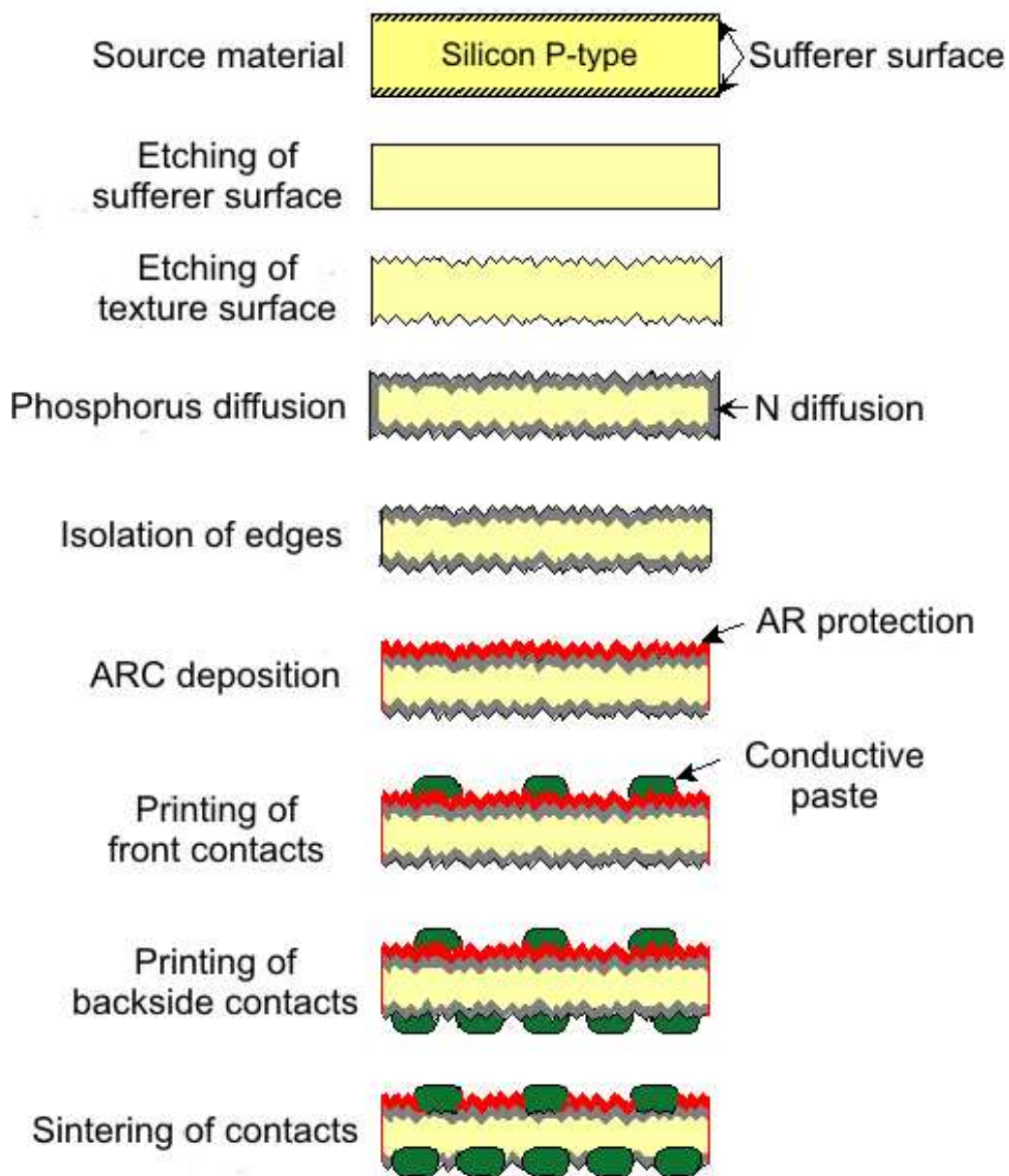


Fig. 4.1: The production P-N junction of solar cells

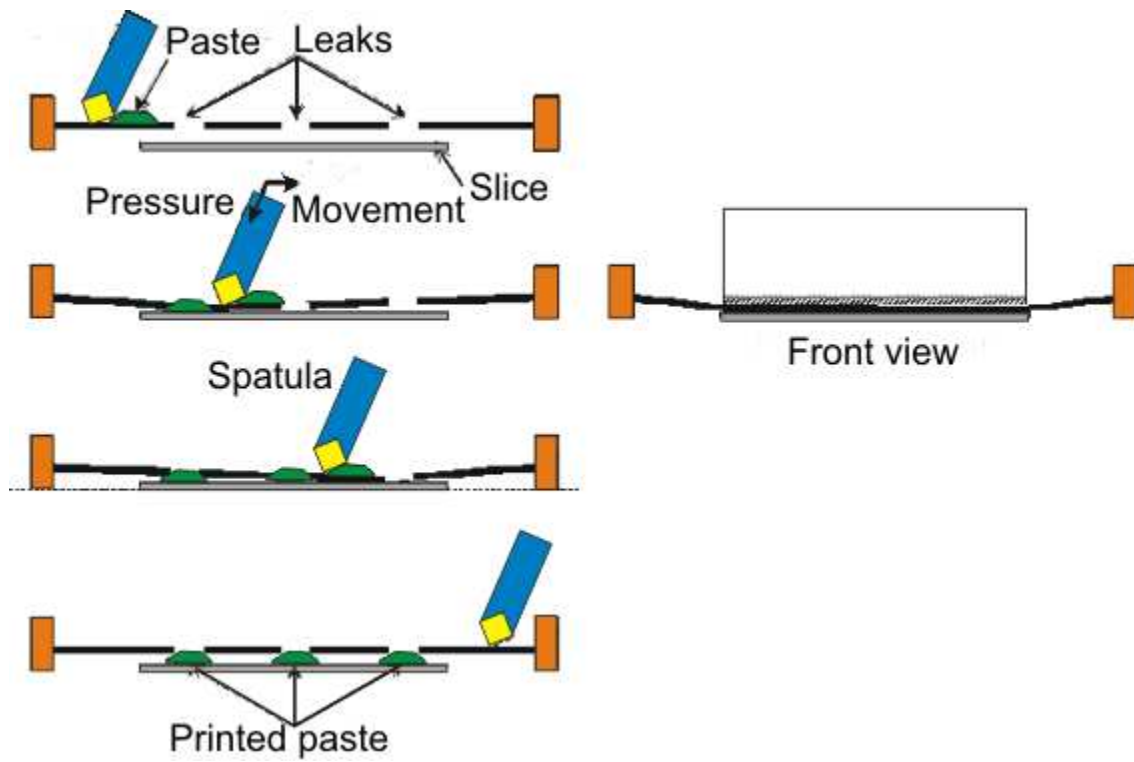


Fig. 4.2: The production of contacts by screen-printing



Fig. 4.3: Polycrystalline, square solar cell

5 SIMULATION OF SOLAR CELL

5.1 Dependence of temperature on the width of the band gap

With increasing temperature, the width of the band gap narrows (see Fig. 5.1). This hypothesis comes out from the fact, that with increasing temperature (increased heat energy) atoms vibrate more and the distances between them increases. This effect is calculated by coefficient of linear expansion. Bigger inter-atomic arrangement lowers the potential of linkages, which narrows the width of the band gap.

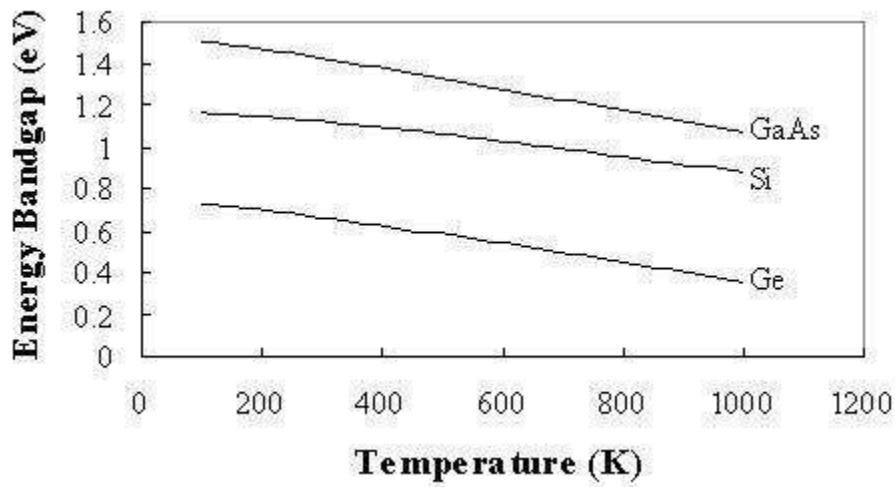


Fig. 5.1: Dependence of band gap width on temperature

A constant temperature of 25°C was assumed for all equations. It was mentioned, that the characteristics change with the temperature. This equation describes how to modify dependence of width of the band gap E_g on the changing temperature:

$$E_g(T) = E_g(0) - \frac{\alpha T^2}{T + \beta} \quad (3)$$

Where: E_g , α , β Fixed values

In following table the size of these values can be seen for silicon, germanium and GaAs compound. (See Table 5.1)

Table 5.1: The fixed values of constants for calculating

	Germanium	Silicon	GaAs
$E_g(0)$	0.7437	1.166	1.519
α (meV / K)	0.477	0.473	0.541
B (K)	235	636	204

An example for calculating the width of the band gap at 300 K:

$$E_g(300K) = E_g(0) - \frac{\alpha T^2}{T + \beta} = 1,166 - \frac{0,473 \cdot 10^{-3} \cdot (300)^2}{300 + 636} = 1,12 eV \quad (4)$$

For completeness in Table 5.2 there are mentioned several values used for calculating width of forbidden bands for the various materials at different temperatures. As can be seen, the band gap width decreases with temperature. [5]

Table 5.2: The width of forbidden bands for different materials at different temperatures

	Germanium [eV]	Silicon [eV]	GaAs [eV]
T = 300K	0.66	1.12	1.42
T = 400K	0.62	1.09	1.38
T = 500K	0.58	1.06	1.33
T = 600K	0.54	1.03	1.28

5.2 Solar cell from an electronic perspective

This simple equivalent circuit of the extended one-diode model (see Fig. 5.2) is sufficient for most applications. Whole chapter is based on the works [1], [6]. Differences between measured and calculated characteristics of the real solar cell are less than few percent.

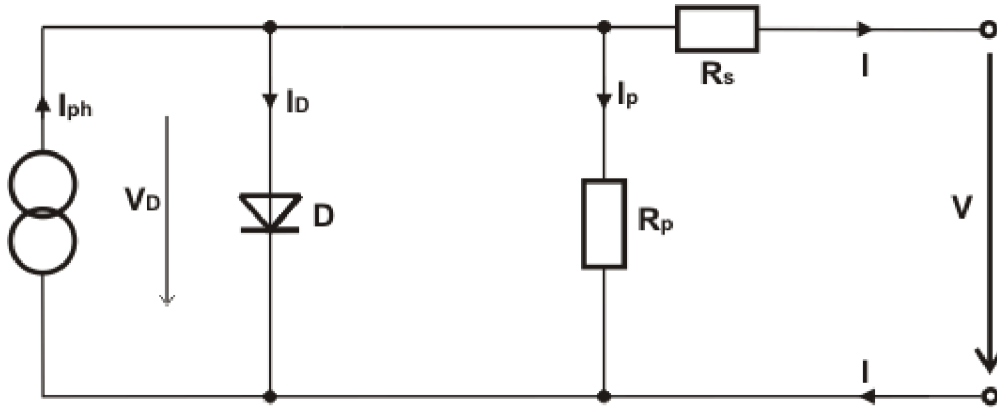


Fig. 5.2: Extended equivalent circuit of a solar cell (one-diode model)

Mathematical expression of this model is:

$$I = I_{ph} - I_S \left(\exp\left(\frac{V + IR_S}{mV_T}\right) - 1 \right) - \frac{V + IR_S}{R_p} \quad (5)$$

Current-voltage characteristics of P-N junction of photovoltaic cell are also affecting by series resistance R_S and parallel resistance R_p . The origins of the series parasitic resistance are based on the overall resistance of semiconductor materials and substrate, defect in the technology, resistance of conductivity contacts and wiring. Parallel parasitic resistance may be caused by extensive defects of crystal lattice, or leakage current around the edges of the cell. Extensive crystal lattice defects, which occur frequently in low-cost semiconductors, are dislocations, grain boundaries and large precipitates.

Effect of size of the series resistance of current-voltage characteristics of solar cell can be seen in the Fig. 5.3. In the Fig. 5.4 can be seen an influence of changing the size of the parallel resistance on the current-voltage characteristics of solar cell.

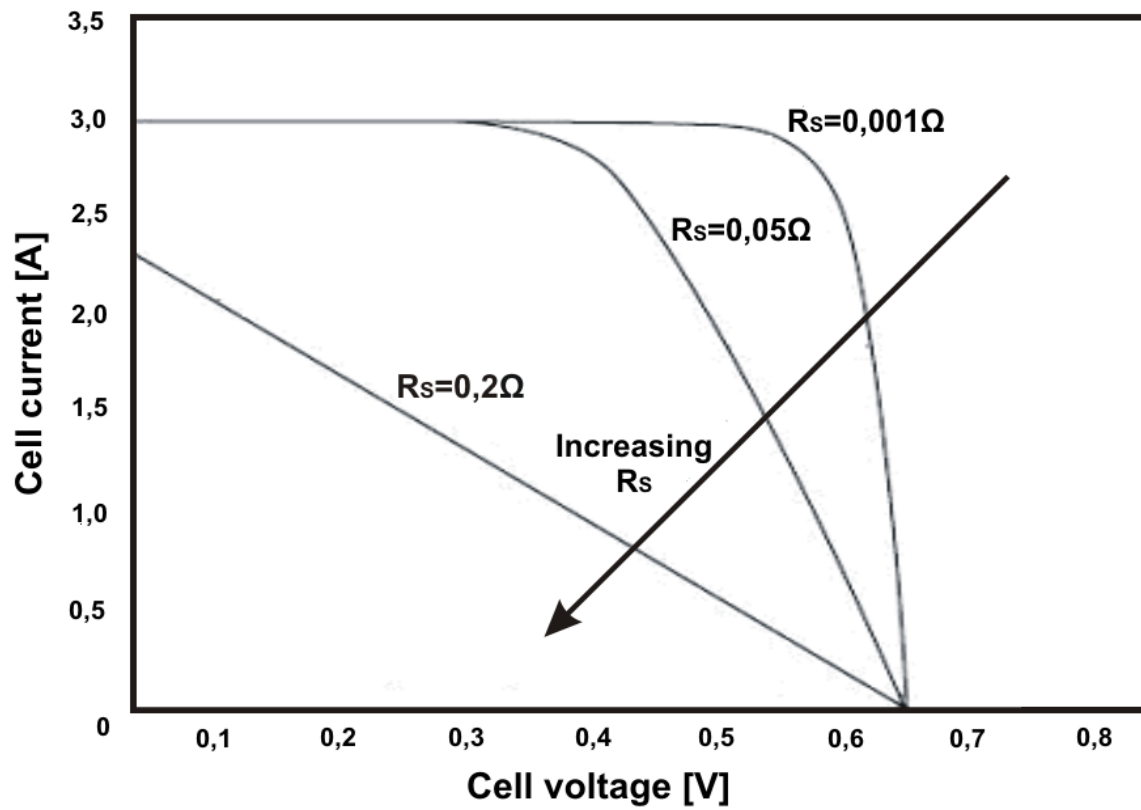


Fig. 5.3: Influence of the series resistance R_s to I-V characteristics of solar cell

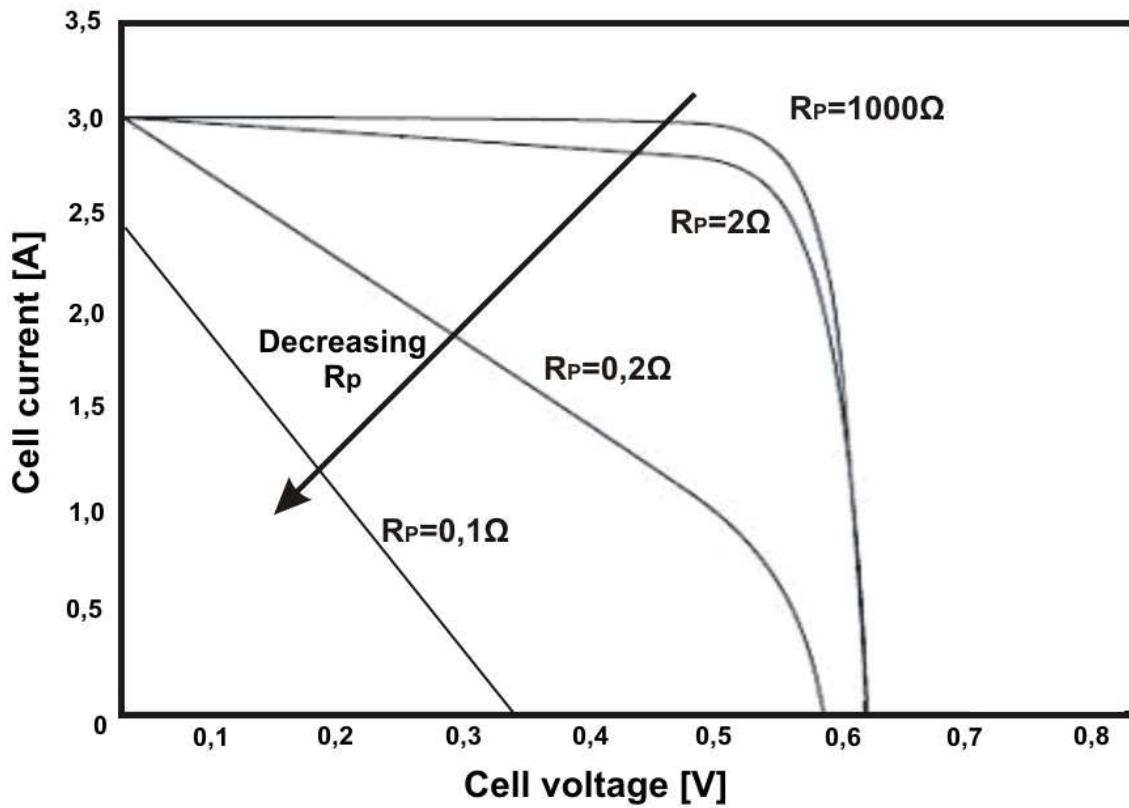


Fig. 5.4: Influence of the parallel resistance R_p to I-V characteristics of solar cell

Fig. 5.3 shows the effect of series resistance on the I-V characteristics. There is evident, that whereby the smaller is the value of the series resistance, the better the I-V characteristic is achieved (the shape of I-V characteristic will be “more rectangular”). When the value of series resistance is equal or this value is higher than 0.2Ω , the classical rectangular I-V characteristics was not obtained, due to large influence of parasitic resistance (is obtained characteristic of resistance). The situation is similar with parallel resistance, but exactly the opposite. Whereby the greater the value of the parallel resistance is, the better the I-V characteristics is obtained. At low resistance values, respectively 0.1Ω , or 0.2Ω was the influence on I-V characteristic so significant, that it is practically just the characteristics of resistance. Incomparably better results will be obtained, if the two-diode model of a solar cell is used. See wiring of two-diode model in Fig. 5.5. Both diodes have different saturation currents and diode factors. Two-diode model is described on the relationship:

$$I = I_{ph} - I_{S1} \left(\exp\left(\frac{V + IR_s}{m_1 V_T}\right) - 1 \right) - I_{S2} \left(\exp\left(\frac{V + IR_s}{m_2 V_T}\right) - 1 \right) - \frac{V + IR_s}{R_p} \quad (6)$$

Where: m_1 Diode factor of the first diode (in ideal diode $m_1 = 1$)

m_2 Diode factor of the second diode (in ideal diode $m_2 = 2$)

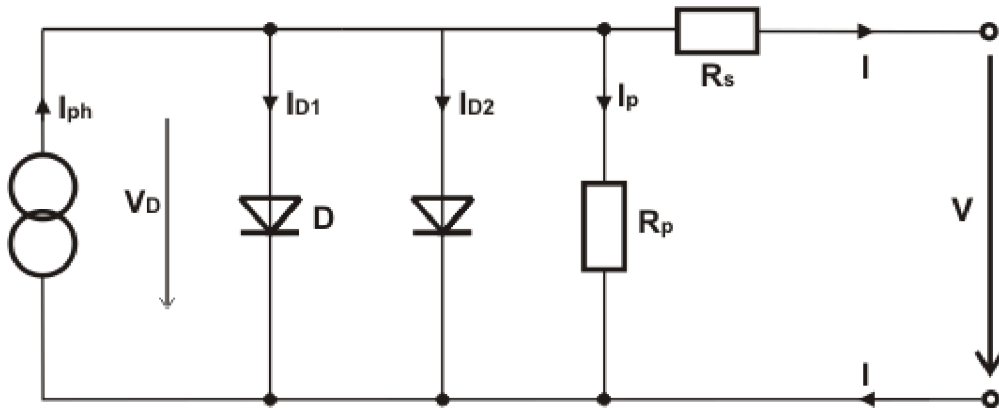


Fig. 5.5: Extended equivalent circuit of a solar cell (two-diode model)

5.3 Parameters of solar cell at light

It is necessary to define others variables which will be used. This section describes the most important and most common parameters [6]:

The voltage of a short-circuited solar cell is equal to zero in the case that the short circuit current I_{SC} is approximately equal to the photocurrent I_{ph} . Since the photocurrent is proportional to the irradiance E , the short circuit current also depends on the irradiance:

$$I_{SC} \approx I_{Ph} = C_0 E \quad (7)$$

Note: C_0 is some coefficient (constant). This equation in simulation is not used, so this constant is not described anymore.

With increasing temperature, the short circuit current rises. The standard temperature for measuring short circuit currents I_{SC} is usually $\vartheta = 25^\circ\text{C}$. The temperature coefficient α_{ISC} of the short circuit current allows its value to be estimated at other temperatures. The relationship for conversion is then:

$$I_{SC}(\vartheta_2) = I_{SC}(\vartheta_1)(1 + \alpha_{ISC}(\vartheta_2 - \vartheta_1)) \quad (8)$$

Note: The temperature coefficient for silicon panel is around the value $\alpha_{ISC} = (10^{-3} \text{ to } 10^{-4})/^\circ\text{C}$

If the cell current I is equal to zero, the solar cell behaves like it is in open circuit operation. The cell voltage becomes the open circuit voltage V_{OC} :

$$V_{OC} = mV_T \ln\left(\frac{I_{SC}}{I_S} + 1\right) \quad (9)$$

Since the short circuit current I_{SC} is proportional to the irradiance E , the open circuit voltage V_{OC} dependence is proportional to the logarithm E .

The solar panel generates maximum power at a certain voltage. Fig. 5.6 shows the dependence of current on voltage as well as the power–voltage characteristic. It shows that the power curve has a point of maximum power. This point is called the maximum power point MPP. The voltage at the MPP, V_{MPP} , is less than the open circuit voltage V_{OC} , and the current I_{MPP} is lower than the short circuit current I_{SC} . The MPP current and voltage are dependent on

irradiance E and temperature T , like as the short circuit current I_{SC} and open circuit voltage V_{OC} . The maximum power P_{MPP} is:

$$P_{MPP} = V_{MPP} I_{MPP} \prec V_{OC} I_{SC} \quad (10)$$

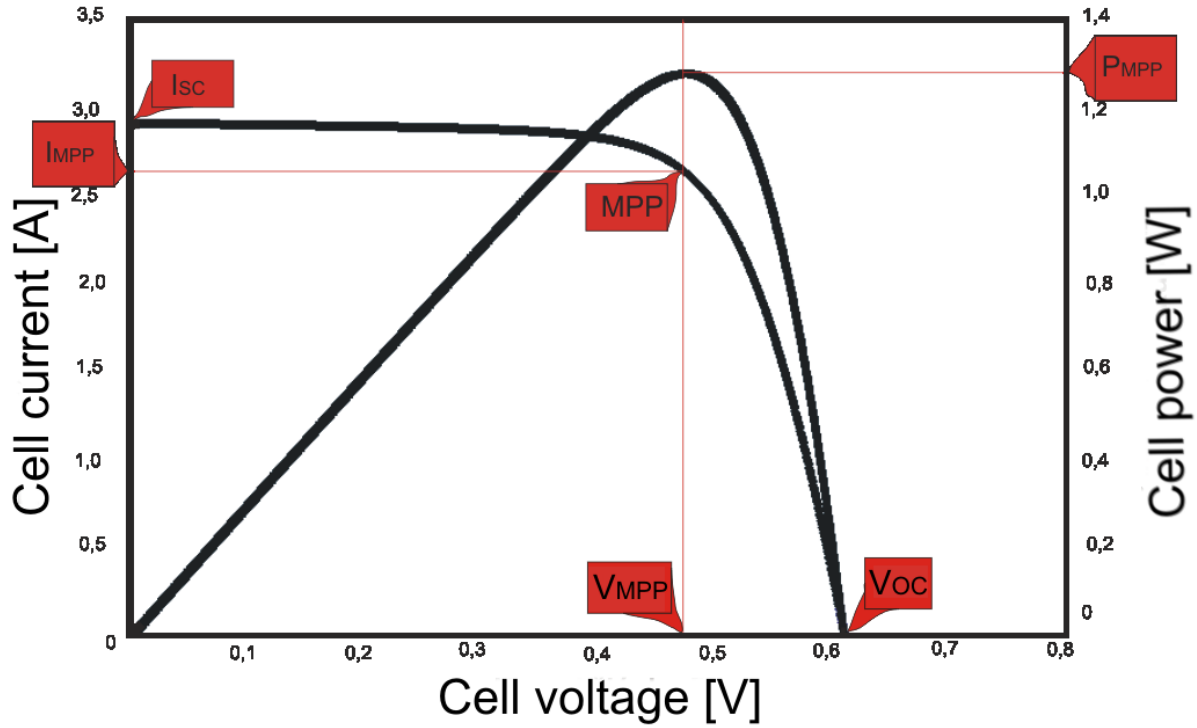


Fig. 5.6: I-V and P-V characteristics of solar cell with maximum power point P_{MPP}

Taking into account the dependence of irradiance in the behaviour of a solar cell, the biggest dominant influence will be influence of current and therefore power dependence P_{MPP} is almost directly proportional to the irradiance E . Because the temperature coefficient of the open circuit voltage α_{VOC} is greater than the actual one, the temperature coefficient of performance α_{PMP} is negative. For silicon cells, the value α_{PMP} is around the value from $-3 \cdot 10^{-3}/^{\circ}\text{C}$ to $-6 \cdot 10^{-3}/^{\circ}\text{C}$. Increasing the temperature by 25°C causes a power drop of about 10%. It is possible to see more in the chapter *Influence of temperature*. To be able to compare the real solar cells to the simulated models, it is an unwritten condition that the MPP is measured under standard conditions (STC), where $E = 1000 \text{ W/m}^2$, $\theta = 25^{\circ}\text{C}$.

Power generated by solar panels, is usually smaller under normal conditions (weather), than the theoretical conditions. For this reason, STC has its own power unit Wp (Wattpeak). Another parameter is the fill factor (FF):

$$FF = \frac{P_{MPP}}{V_{OC}I_{SC}} = \frac{V_{MPP}I_{MPP}}{V_{OC}I_{SC}} \quad (11)$$

Fill factor is the criterion of quality solar cells, which describes how well, the I-V curve fits into the rectangle formed by the V_{OC} and I_{SC} . Its value is always less than 1. If the value is 1, the curve will be totally rectangular, which is not possible. Normally the value is between values 0.75 to 0.85. All the above-mentioned components together, the MPP power P_{MPP} , the irradiance E and the solar cell area A describe the efficiency of solar cell η :

$$\eta = \frac{P_{MPP}}{EA} = \frac{FF \cdot V_{OC} \cdot I_{SC}}{EA} \quad (12)$$

Efficiency is usually determined under standard test conditions. The following Table 5.3 is a summary of the different parameters of solar cells:

Table 5.3: Important electrical solar cell parameters

Name	Symbol	Unit	Note
Open circuit voltage	V_{OC}	V	$V_{OC} \sim \ln E$
Short circuit current	I_{SC}	A	$I_{SC} \approx I_{ph} \sim E$
MPP voltage	V_{MPP}	V	$V_{MPP} < V_{OC}$
MPP current	I_{MPP}	A	$I_{MPP} < I_{SC}$
MPP power	P_{MPP}	W or W_p	$P_{MPP} = V_{MPP} \cdot I_{MPP}$
Fill Factor	FF	-	$FF = P_{MPP} / (V_{OC} \cdot I_{SC}) < 1$
Efficiency	η	%	$\eta = [P_{MPP} / (E \cdot A)] \cdot 100$

5.4 Influence of temperature

Constant temperature 25 °C was used in all equations of the previous section. All the characteristics are changing with changing temperature. This section describes dependence of temperature on I-V characteristic of the solar cell.

The thermal voltage must be calculated for a given temperature. Absolute temperature: T [K] ($T = \vartheta (K/^{\circ}C) + 273.15$ K). Thermal voltage is given by this equation:

$$V_T = \frac{kT}{e} \quad (13)$$

Where: Boltzmann constant $k = 1.380658 \cdot 10^{-23}$ J/K

Elementary charge $e = 1.60217733 \cdot 10^{-19}$ A•s

Saturation currents I_{S1} and I_{S2} and width of band gap E_G are also dependent on temperature. For these variables apply the following relations:

$$I_{S1} = C_{S1} T^3 \exp\left(-\frac{E_G}{kT}\right) \quad (14)$$

$$I_{S2} = C_{S2} T^{\frac{5}{2}} \exp\left(-\frac{E_G}{2kT}\right) \quad (15)$$

Note: For one-diode model is used only the equation (14). For two-diode model are used both equations, respectively equations (14) and (15).

These equations ignore the temperature dependence of the width of the band gap. The temperature does not have a significantly influence on the saturation currents and has a decisive influence on the photocurrent I_{Ph} . Due to the narrowing the width of the band gap with increasing temperature, photons with lower energy can elevate electrons into the valence band, which increases the photocurrent. When the coefficients C_1 and C_2 are used, the temperature dependence of the photocurrent is given by equation:

$$I_{Ph}(T) = (C_1 + C_2 T) E \quad (16)$$

Note: It is possible to see more about coefficients C_1 and C_2 in the chapter SEARCHING CONSTANTS OF SOLAR PANEL.

Fig. 5.7 shows the I-V characteristics with various temperatures ϑ . It shows clearly that the open circuit voltage V_{OC} decreases significantly, when the temperature rises. On the other hand, the short circuit current I_{SC} slightly increases. [6]

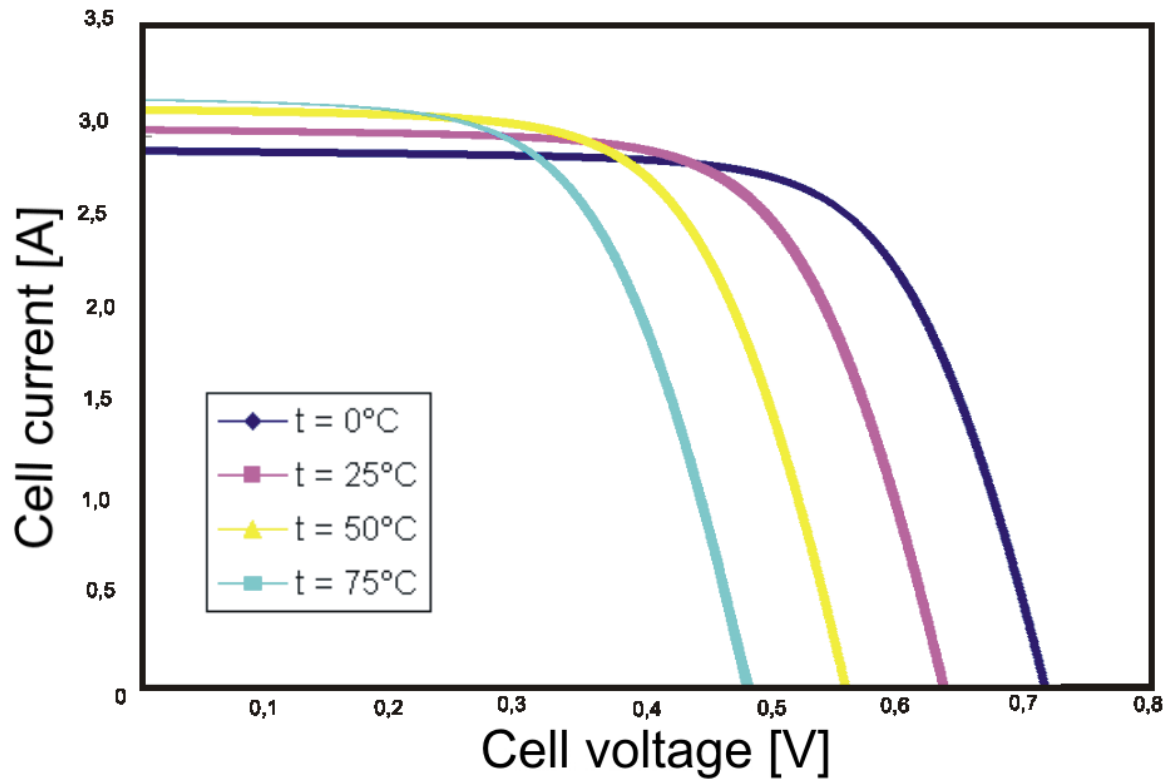


Fig. 5.7: I-V characteristics of the temperature dependence on solar cells

5.5 Series and parallel connections of solar cells

I-V characteristic of the photovoltaic cell is also affected by a series resistance R_s and a parallel resistance R_p . Series parasitic resistance in the real measurement refers to the total resistance of semiconductor materials, the resistance of contacts and wiring. Parallel parasitic resistance is caused by crystal lattice defects, or leakage around the edges of the borders of the solar cell.

Solar cell in normal conditions, does not work separately because of their low voltage. By joining these cells in series, parallel or series-parallel configuration photovoltaic system is created (solar panel). When solar cells are connected in series link, it increases voltage. In the parallel configuration increases the value of current. Most cells are designed to work with 12 V rechargeable batteries. The optimum number of joined silicon solar cells is between 32 and 40. Fig. 5.8 shows the series connection of photovoltaic solar cells:

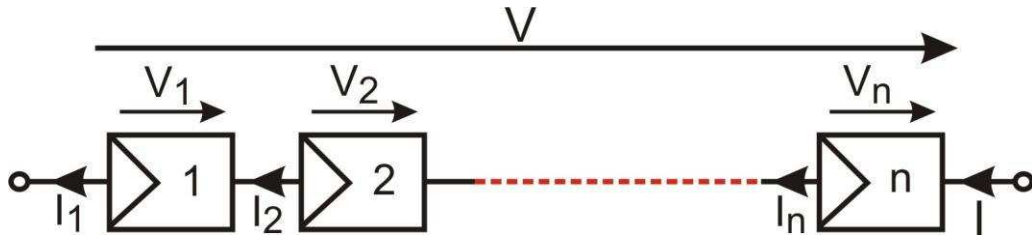


Fig. 5.8: Series connection of photovoltaic solar cells

The first Kirchhoff's law gives us the relationship:

$$I = I_1 = I_2 = \dots = I_n \quad (17)$$

Suppose that all cells are identical and all cells are same irradiated, they have the same temperature and the total voltage is then expressed by the following equation:

$$V = \sum_{i=1}^n V_i \quad (18)$$

In Fig. 5.9, there are the characteristics of single cells. It is possible to see I-V characteristic for any series connection.

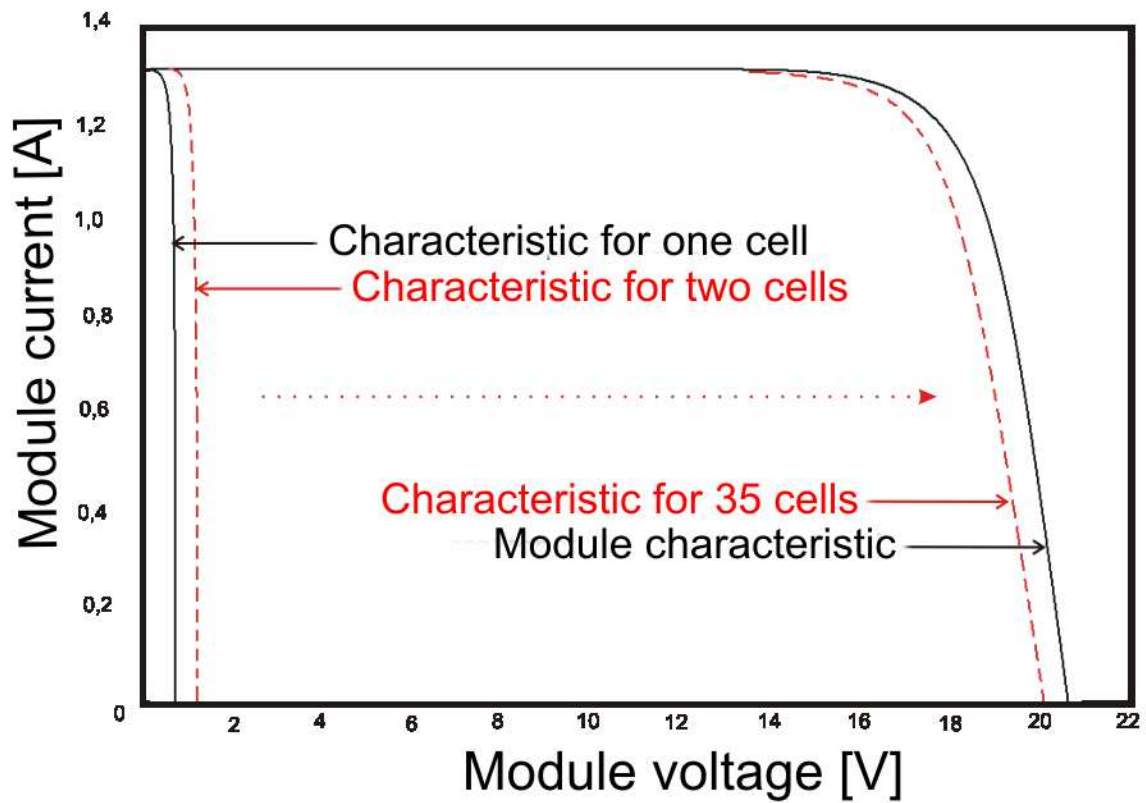


Fig. 5.9: I-V of the solar panels up to 36 potential cells in the series connection

Parallel connection of solar cells is also possible. Practical use it is not as common as in the series connection. In the parallel connection there are higher losses in the transmission of energy. Parallel connection is shown in Fig. 5.10. [6]

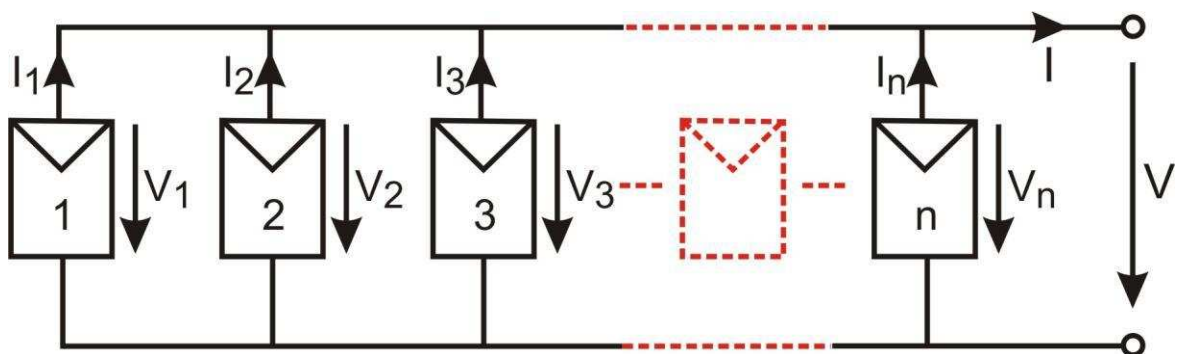


Fig. 5.10: Parallel connection of n photovoltaic solar cells

6 SIMULATION

6.1 The programming environment

The program VEE Pro 8.0 is graphical programming software of Agilent. Programming language uses a graphical display similar to the flow diagram. It is relatively easy to learn to work with Agilent VEE software, and you can start your measurements in a very short time.

6.2 About

The models I-V characteristics of a solar cell were constructed in the program VEE Pro 8.0. One-diode model and also the more accurate two-diode model were simulated in this program. In these models, you can set many different variables. Here, is the full list with the short characteristics:

- Influence of temperature (T). With decreasing temperature, the power increases. The current I_{SC} decreases, but less than the increase of the voltage V_{OC} . (by analogy with increasing temperature, decreases power)
- Intensity of light-irradiance (E). The higher the irradiance is, the higher the power is. Current I_{SC} and voltage V_{OC} are growing with increasing intensity of light.
- Area of the cell (A). With larger contact area, obviously the cell achieves greater power. Raising the voltage and mainly the current.
- Diode factor (m). According to theoretical presumptions, in an ideal one-diode model, the value of diode factor equals to 1. In real measurements, this value can reach values in the range of 1 to 5. In real measurement of two-diode model, the first diode factor m_1 is equal to 1 and the second diode factor m_2 equals 2. For the experimental trials, the first diode factor kept changing in the interval of 1 to 5 and the second diode factor in the range of 2 to 5.
- Series resistance R_S . With increasing series resistance decreases power and worsens FF. The lower the series resistance, the better characteristics are achieved. (Higher value of power and higher FF are achieved).
- Parallel resistance R_P . Influence on the I-V characteristic is not as noticeable as in the case of influence of series resistance. With decreasing resistance, decreases power. Again, the greater the parallel resistance is, the better results we achieved.

- Number of series connected cells. When the number of series-connected cells is increased, it results in increased power. With that series connection, it increases the value of voltage.
- Number of parallel connected cells. When the number of cells linked in parallel is increased, it increases power. With that parallel connection, it increases the value of current.

6.3 Graphic design

Graphic design for one-diode model (see Appendix A), and two-diode model (see Appendix B) is clear and intuitive. There are "sliders" with the necessary values, which were discussed in the previous sub-chapter (such as the effect of irradiance, series resistance, etc.). The scroll bars can easily change these values to another desired value. The necessary information is clearly visible on the screen, such as open circuit voltage V_{OC} , short circuit current I_{SC} , voltage V_{MPP} (voltage at maximum power), current I_{MPP} (the value of current at maximum power), the number of cells, power of system P_m , fill factor FF , and the efficiency of solar panel η . For the comfort for the user, there is an important button called Excel. It push exports all necessary data to Microsoft Excel table. Potentially useful graphs are generated also in Microsoft Excel. The main screen is dominated by two graphs. The first (upper) generates I-V characteristics of solar cell and solar cell P-V characteristics. Also these graphs are generated for solar panels (series, parallel or series-parallel connection configuration of solar cells). The second (lower) chart shows the currents calculated for each step. It is possible to set constants C_{S1} , C_{S2} , C_1 and C_2 , which describe the characteristics of individual solar cells.

6.4 Programmatic design

The models are described by mathematical equations. The one-diode model (see equation (5)) and two-diode model (see equation (6)) are transcendental. Therefore, the equations do not have algebraic solutions, but only numerical. Unknown variable, namely the current I , cannot spin off on one side of the equation, so it is necessary to solve this equation by numerical methodology. There have been used two different ways to obtain the right results. The first method that has been tried is called "Incremental method". For each value of voltage (from the value 0, case B, to V_{OC} , case A) it finds the "correct" value of the current I .

In the first step, each value of current I is set to zero (case C) and is calculated with the appropriate equation for the model (for one-diode model it is equation (5), for two-diode model it is equation (6), case D). After calculating the equations, it is obtained the new calculated value of current I (case E). This value feedback is returned to the appropriate equation (case F) until the value of current converges so that the difference in values of the neighbouring currents is less than the given constant k (case G), then the value of current is recorded (case J) and all the algorithm is repeated with the next incremental value of the voltage (case L). In our case, the value of the constant k is set to 0.001. In the event that the value of the current is not converged even after 50 iterative steps (case H), the proper value of the current is determined by the value of the average currents of the first two measurements (case I) and the value is recorded (case K). In this case, it is an inaccurate measurement, or rather a rough estimate of the value of the current. After finding our desired current for the voltage, the next step is to increment the value of the voltage (case L) and the process is repeated. With this fundamental principle, we can identify all the points, which are needed to render the I-V characteristic. This model is illustrated in Fig. 6.1.

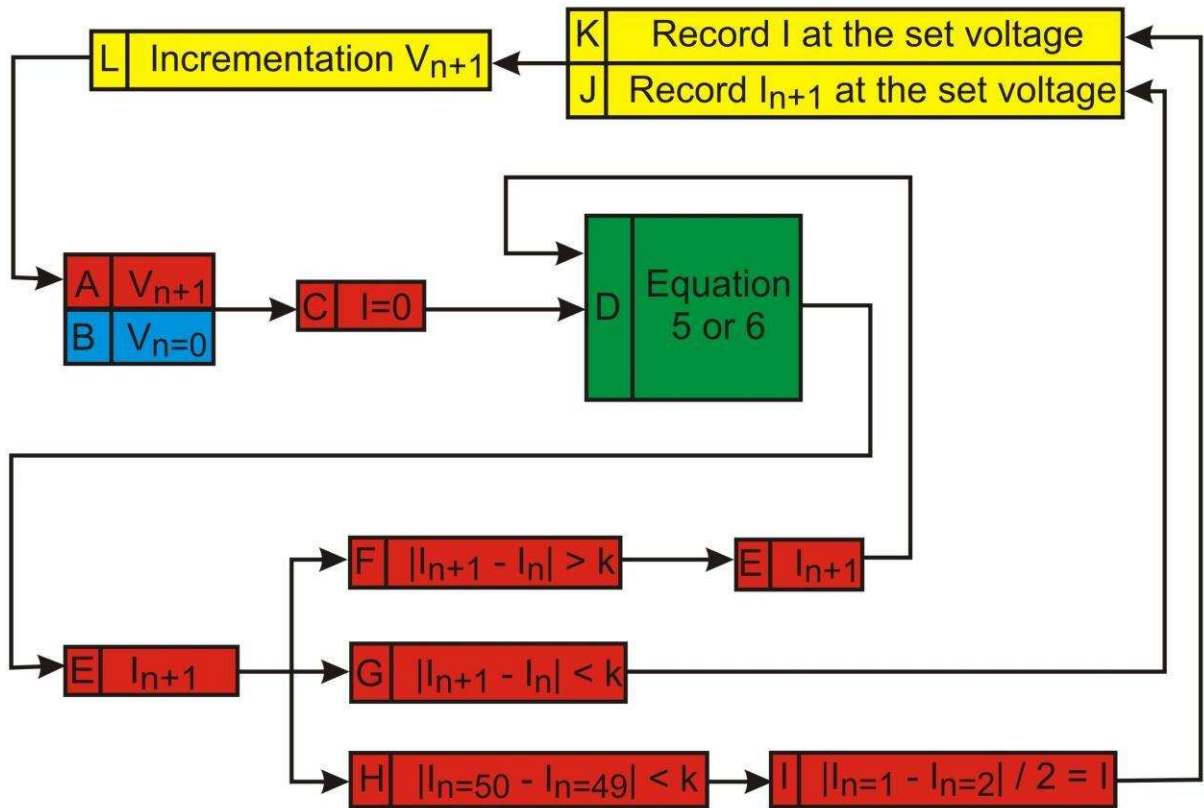


Fig. 6.1: Block diagram of the incremental method

The model was originally used as the “basic building block”. From the test simulations it was found, that the set of extreme values (such as high series resistance or low temperature), this method fails. With growing value of calculated voltage, the current ceases to converge and cannot accurately determine the appropriate current value. See in Fig. 6.2.

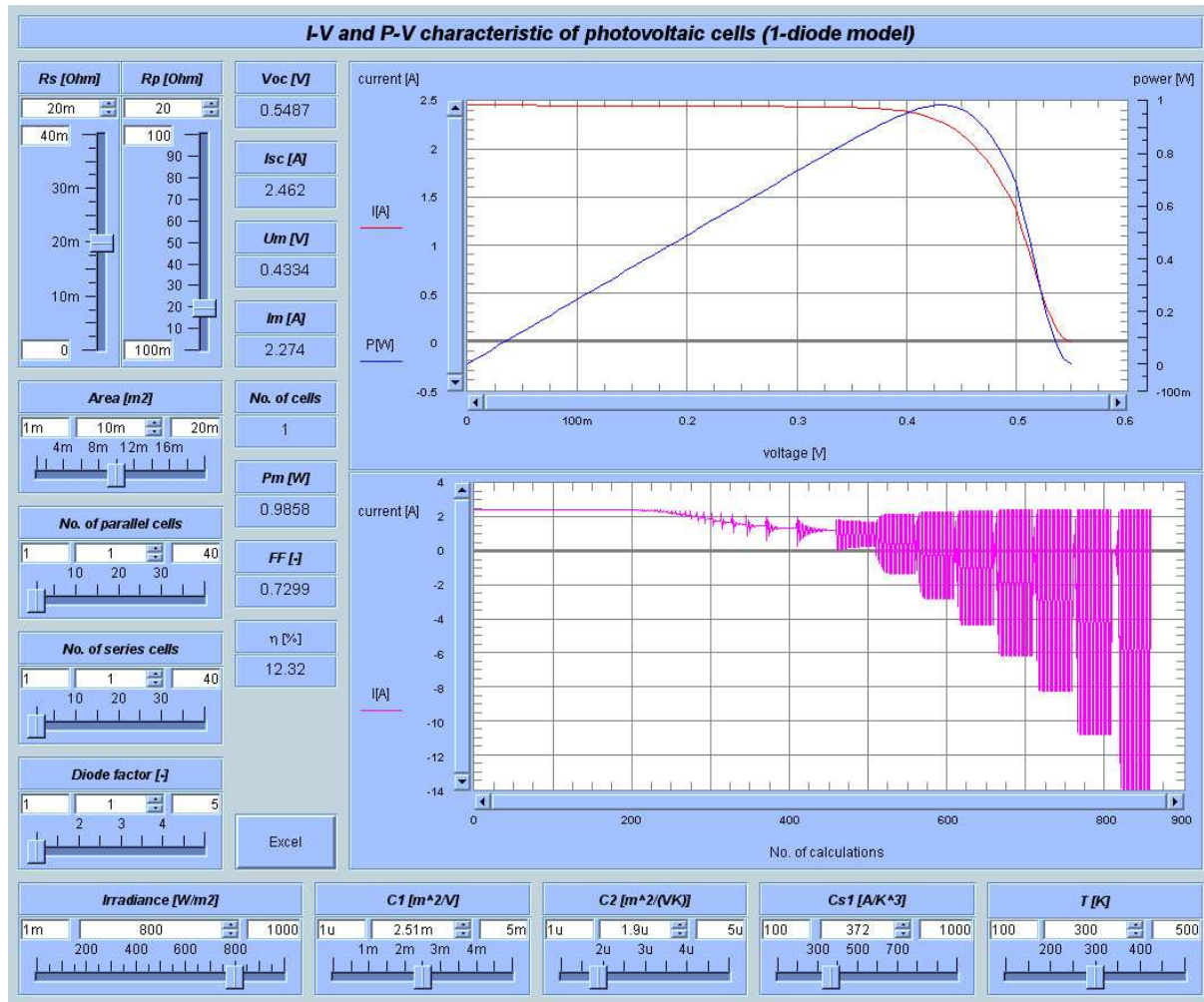


Fig. 6.2: Operational screen of one-diode model for the program using incremental method

Note: In the top of the screen the I-V characteristic of the graph shows, that the incremental numerical method fails. I-V characteristic crashes especially at high voltage V. The bottom graph shows the current divergence in the calculation. This method in extreme input parameters fails, because the calculated flow ceases to converge (see the details above).

For this reason, to calculate the corresponding current there was used another method called "interval method". In the beginning it is important to calculate the value of I_{Ph} (case C). The value of I_{Ph} is calculated only for the case that value of voltage $V = 0$ and this value of I_{Ph} is used also for the next increments of voltage. For each value of voltage (from the value 0,

case B, to V_{OC} , case A) the count 0 (case D) is assigned and the calculated current I_{ph} is divided into ten subintervals from 0 to I_{ph} (case E). The value of the upper boundaries of each subinterval is substituted gradually and directly into the appropriate equation (for one-diode model it is equation (5), for two-diode model it is equation (6), case F). The value Count is incremented by 1 (case G). The resulting value of current I is in the interval from 0 to I_{ph} and the right subinterval is found by the smallest difference (case H) between the input (set) and the obtained calculated (calc) output value of the current. This determined subinterval of current I is then further examined. Thus, the subinterval is divided again into 10 more subintervals (Case I). This process is repeated until the value of Count is less than 4 (Case J), so that the exact determination of the current is $I_{ph}/10^3$. That is why for every value of voltage 30 calculations are made. After all 3 circles the upper boundary of determined subinterval is recorded (Case K) and algorithm continues the process with the next increment of the voltage (Case B). This model is illustrated in Fig. 6.3. In Fig. 6.4 is an operational screen of program, which uses interval method. Here it is seen that this method works well although the user set extreme values. In the future solely interval method will be used.

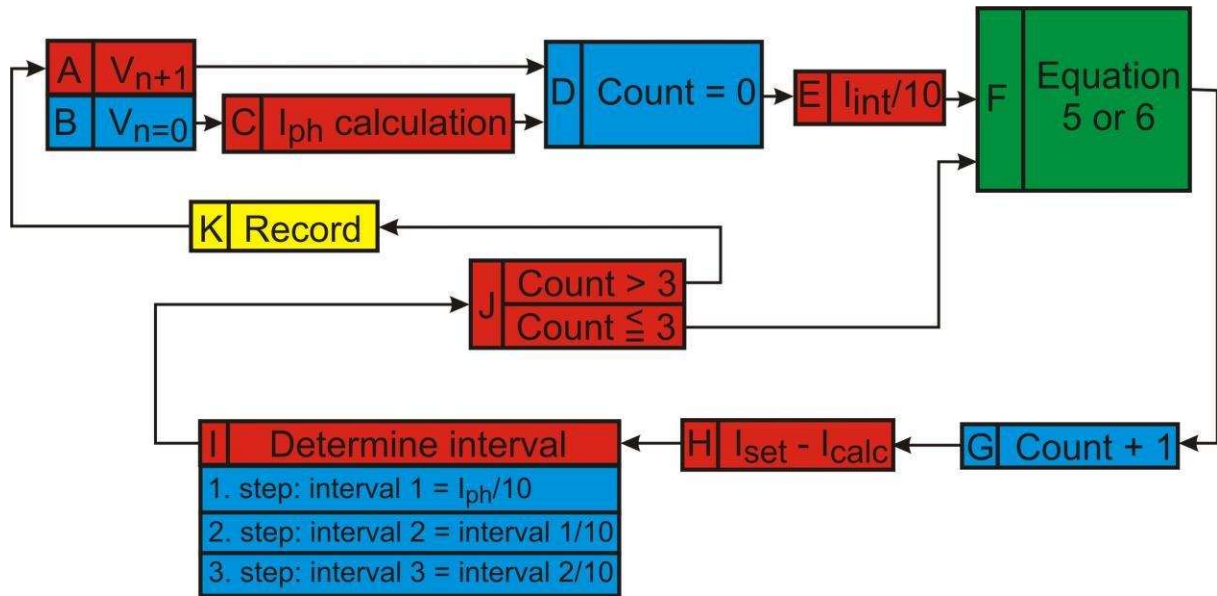


Fig. 6.3: Block diagram of interval method

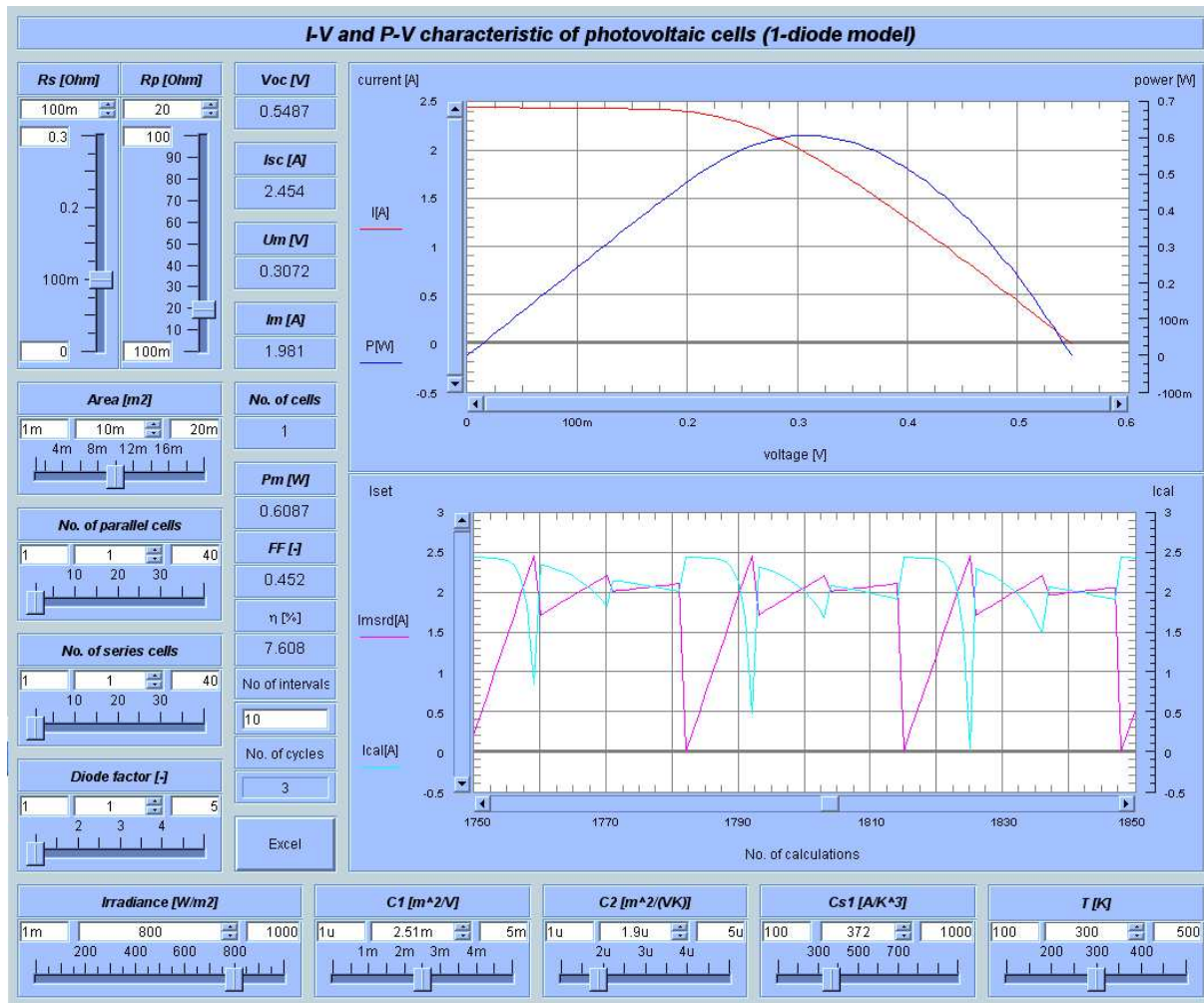


Fig. 6.4: Operational screen of one-diode model for the program using interval method

Note: In the top of the screen, the I-V characteristic of the graph shows that the numerical method works correctly even when you enter extreme input parameters. The bottom graph shows two curves. First curve shows the value of our set currents. The second curve shows the calculated values of currents. Seeking correct value of the current is in the area around the crossing of these curves. After finding this crossing, that region is explored twice again, the precise value is achieved. Thus, for each value of voltage the cycle is performed three times, as it is possible to see from the bottom graph. The Fig. 6.4 shows three results for the value of the currents.

6.5 Example (Incremental method)

There have been set "random" values into this program. See Table 6.1. The resulting values are shown in Table 6.2. Furthermore, graphs of I-V characteristics of solar cells are on Fig. 6.5 (for one-diode model) and Fig. 6.7 (for two-diode model). On the charts, there are also shown significant convergence values of currents at various computational steps. See Fig. 6.6 (for one-diode model) and see Fig. 6.8 (for two-diode model).

Table 6.1: A selection achieved value in the program using the increment method

	Rs [mΩ]	Rp [Ω]	No. of series [-]	No. of parallel [-]	Irradiance [W/m ²]	A [m ²]	D.f. 1 [-]	D.f. 2 [-]	T [K]
one-diode model	14	89.5	6	2	700	1·10 ⁻²	1	-	300
two-diode model	14	89.5	6	2	700	1·10 ⁻²	1	2	300

Table 6.2: The resulting values

	V _{OC} [V]	I _{SC} [A]	V _m [V]	I _m [A]	No. of cells [-]	P _m [W]	FF [%]	η [%]
one-diode model	3.272	4.310	2.650	4.070	12	10.77	76.38	12.86
two-diode model	3.271	4.310	2.620	4.000	12	10.47	74.22	12.46

Note: In Table 5.3 and Table 6.2 there are slight differences in the variables, which are caused by other variables markings from various literary sources. In Anglo-Saxon countries, it is customary to express the point of maximum voltage V_{MPP} (From English Maximum Power Point). In Table 6.2 it is shown as V_m (from the Czech maximum). Therefore, the difference between these two variables does not exist within the sign. Other similar cases of equivalence are those of I_{MPP} which is I_m and P_{MPP} which is the P_m.

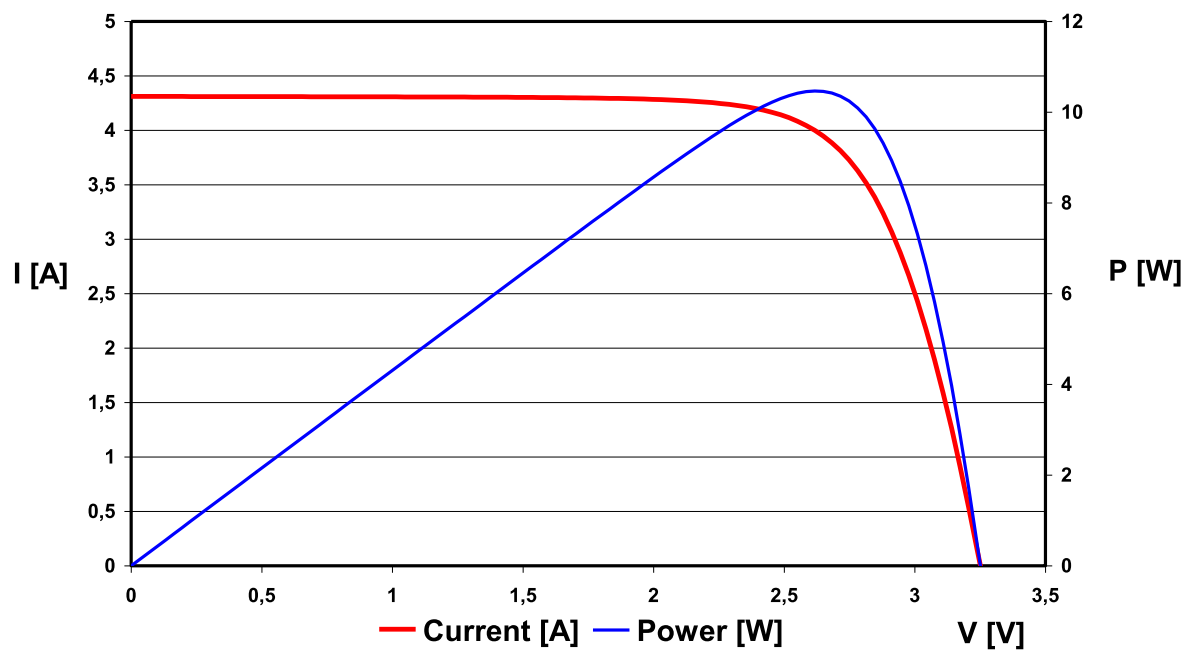


Fig. 6.5: I-V characteristic of one-diode model of the solar panel at random constants (see Table 6.1)

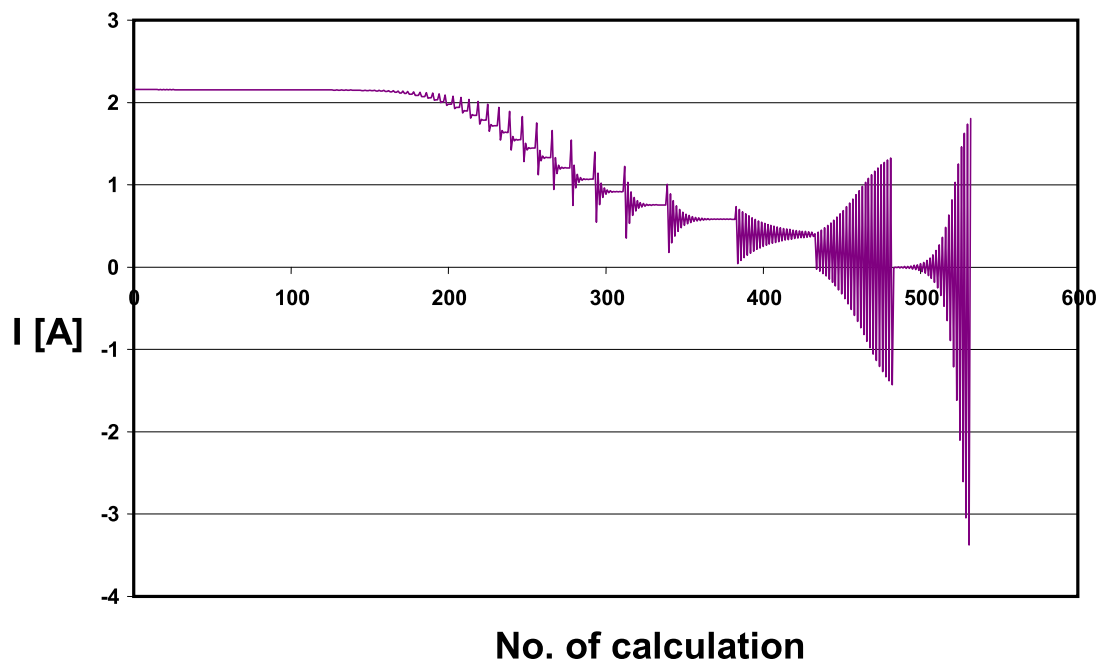


Fig. 6.6: The values of currents at various iterations (one-diode model)

Note: In this chart (see Fig. 6.7) can be seen in the vast majority of cases, when the extreme values of variables are not set, that the value of current I converges to the given conditions before the "limit" of 50 cycles. With increasing value of voltage, converge gets worse. Respectively the last two values diverge. This comes under the second model described in the subchapter Programmatic design (result is given by average of the first two calculated values).

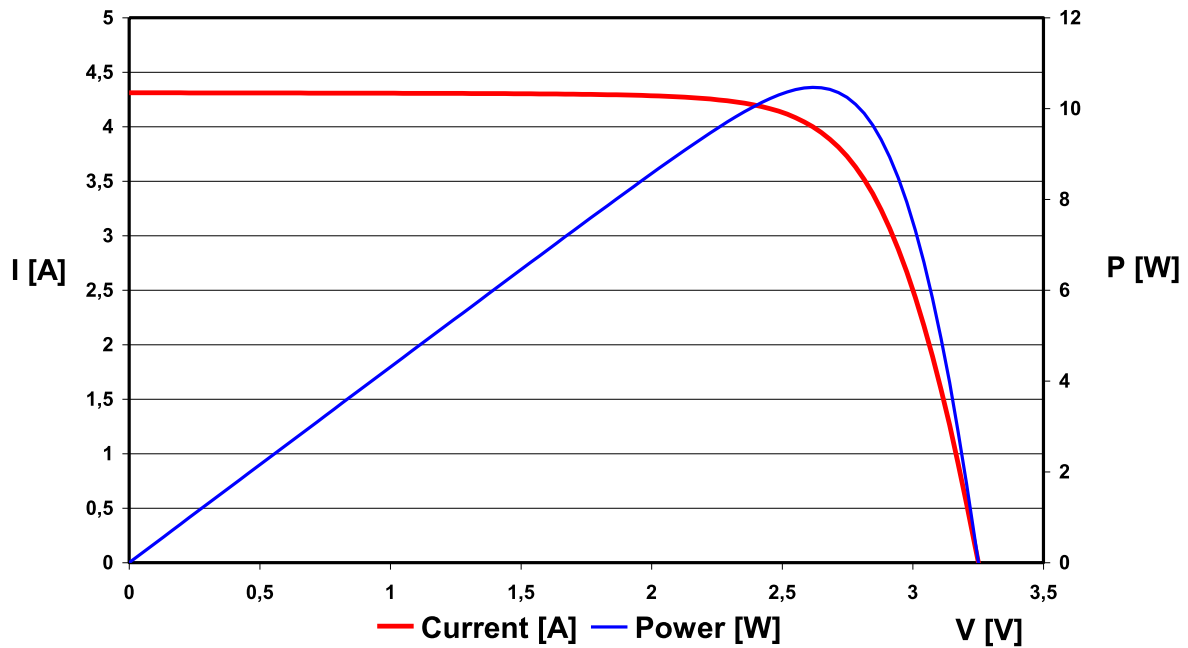


Fig. 6.7: I-V characteristics of two-diode model of solar panel at random values of constants (see Table 6.1)

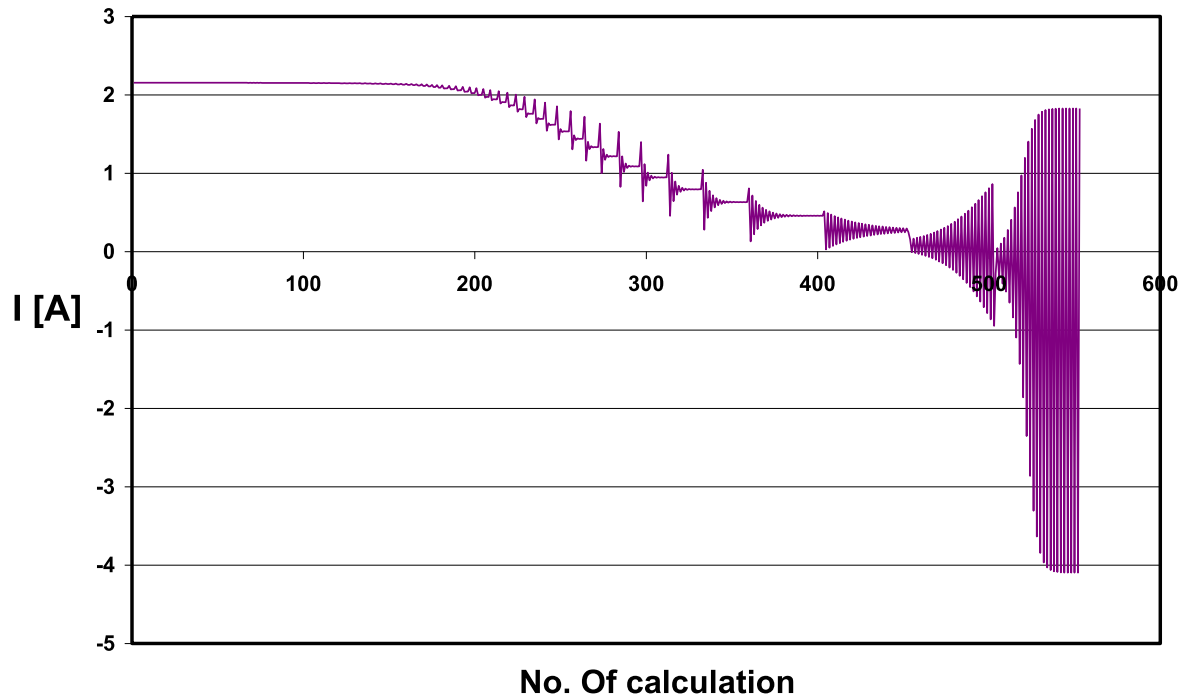


Fig. 6.8: The values of currents at various iterations (two-diode model)

6.6 Temperature and irradiance

Even from the operation screen (e.g. Appendix A) it is possible intuitively to mark out, that we can quite easily see from a visual perspective the number of solar cells and determine how the cells are connected. Possibilities are connections in series, parallel or series-parallel connection. In addition, it is possible to measure the area of this panel. All that it is necessary is to measure the light intensity (irradiance) and the temperature. The measurements were made in a darkened laboratory, using light (150 W halogen lamp) hanging on a sliding stand. Light intensity for different distances of light sources was measured using a fixed Pyranometer and sliding holder of lamp. For a better idea, see Fig. 6.9. Dependence of light intensity on the distance is expressed in Fig. 6.10. Here it is evident, that the intensity of incident light decreases exponentially with distance.

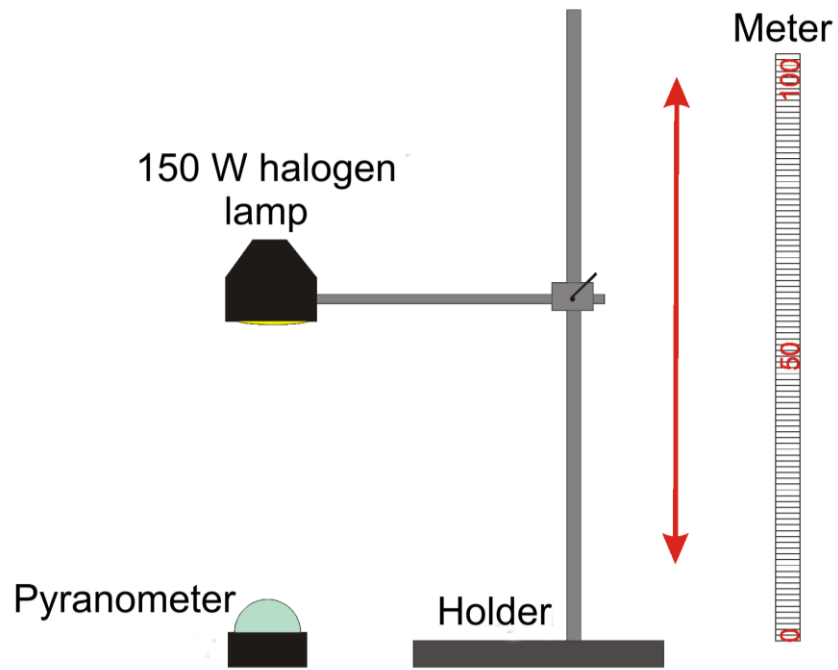


Fig. 6.9: Scheme of measurement irradiance in different distances of source of light

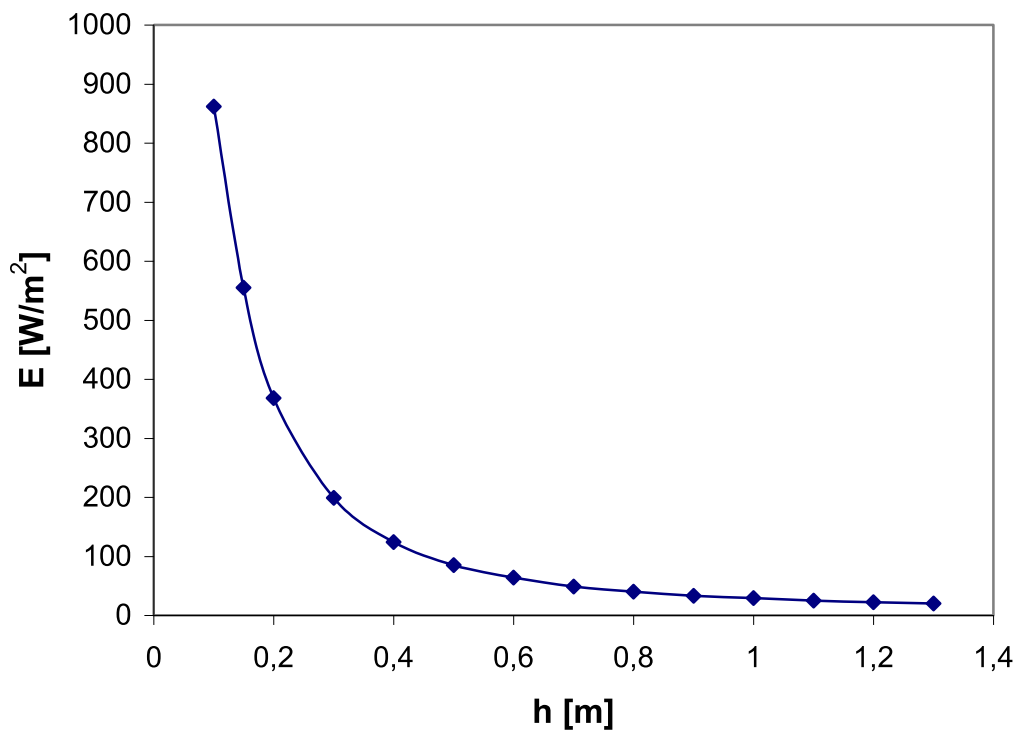


Fig. 6.10: Dependence of light intensity of 150 W halogen lamp on distance from pyranometer

The second parameter is the effect of temperature. This influence on the I-V characteristics of solar cell is very substantial. Temperature measurement was significant for two reasons. The first one is to measure the actual temperature and the second one is to identify the time when it is possible to measure the real I-V characteristic of a solar panel. Since the temperature has great influence on I-V characteristics of the solar panel, so it is important to wait until it reaches a constant temperature. The halogen lamp is held at a distance of $1 \cdot 10^{-1}$ m, $2 \cdot 10^{-1}$ and $4 \cdot 10^{-1}$. In these cases the temperature stabilizes at a time of about 3 hours. See in Fig. 6.11. This measurement is realized using PT100 resistance temperature sensors. Screenshot of program is in Appendix E. Here is used the basic equation to calculate the temperature (19):

$$R_t = R_o [1 + \alpha_R (\vartheta_t - \vartheta_o)] \quad (19)$$

Where: R_o is the resistance at temperature $\vartheta_o = 0^\circ\text{C}$ [Ω]

R_t is the resistance at the current measured temperature ϑ_t [Ω]

α_R is the temperature coefficient of resistance [K^{-1}]

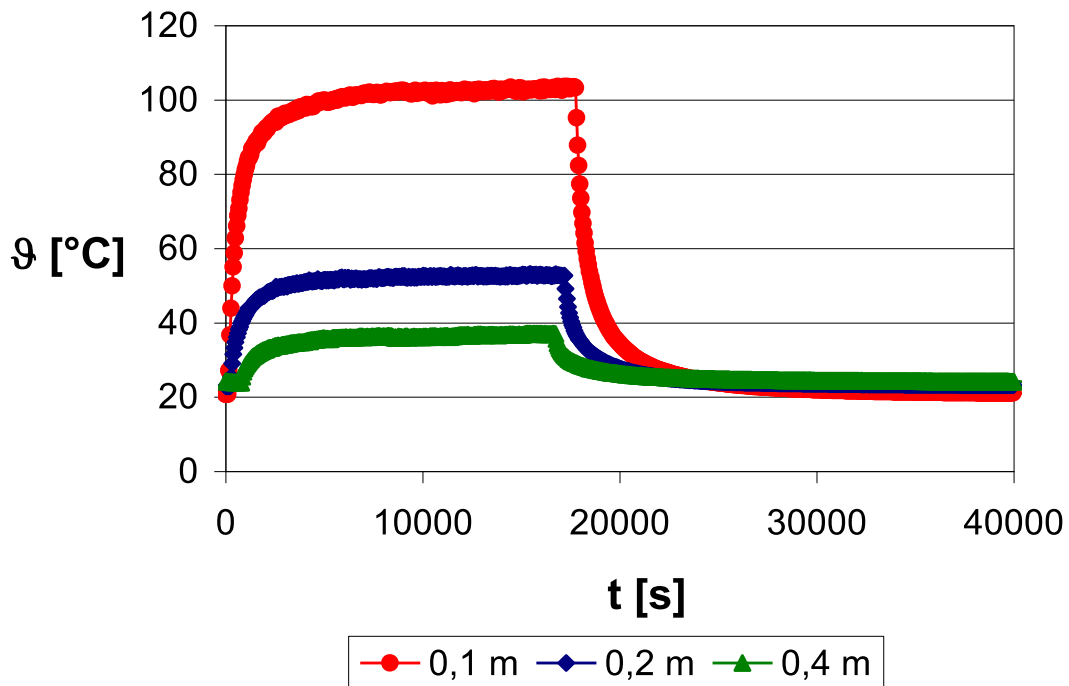


Fig. 6.11: Temperature dependence on time in light 150W halogen lamp at a distance of $1 \cdot 10^{-1}$ m, $2 \cdot 10^{-1}$ m, $4 \cdot 10^{-1}$ m (862 W/m^2 , 368 W/m^2 , 124 W/m^2)

7 MEASUREMENT OF I-V CHARACTERISTIC OF SOLAR PANEL

In this section real measurement of I-V characteristics of the solar panel is made. See wiring diagram in Fig. 7.1. Alternative wiring diagram of I-V characteristics of a solar panel (with computer) is seen in Fig. 7.2. In Fig. 7.3 it is possible to see photo documentation of laboratory measurements. When the panel is irradiated, it is necessary to use load resistance of an order of $100\ \Omega$. In the absence of this resistance, it is not possible to achieve higher voltage setting. Resistance is serially connected with the source. It sets the voltage at the source so that it can measure the voltage on the entire interval from 0 to V_{OC} . A program sets the voltage at the source from computer, which is connected via GPIB cable. In the measurement, it is necessary change polarity by changing lead cables connected with the source, in order to measure the entire I-V characteristic of the solar panel. By Ammeter current I is measured, which is absorbed from the solar panel and Voltmeter is used to measure voltage V in the solar panel. This data is recorded on a computer. Transport of data is realized via USB cable.

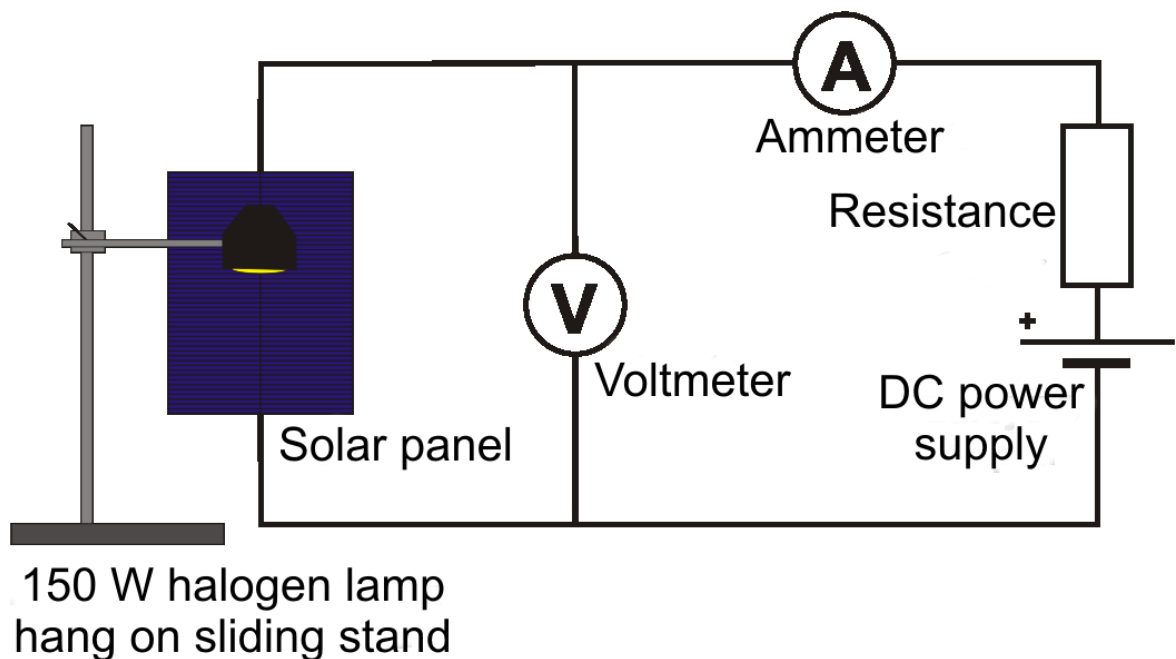


Fig. 7.1: Schematic wiring circuit for the measuring of I-V characteristic of the solar panel

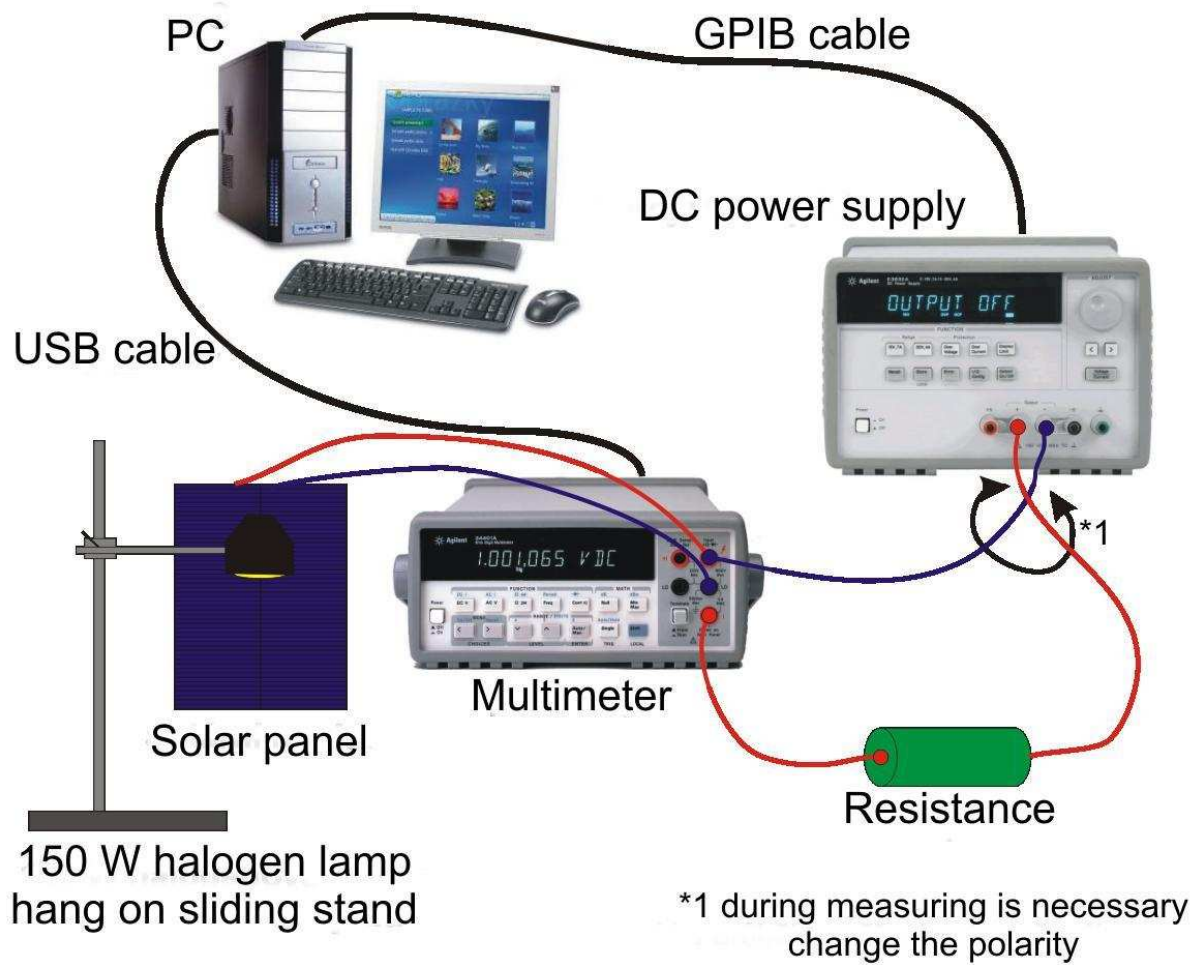


Fig. 7.2: Alternative wiring circuit for measuring I-V characteristic of a solar panel (including computer)

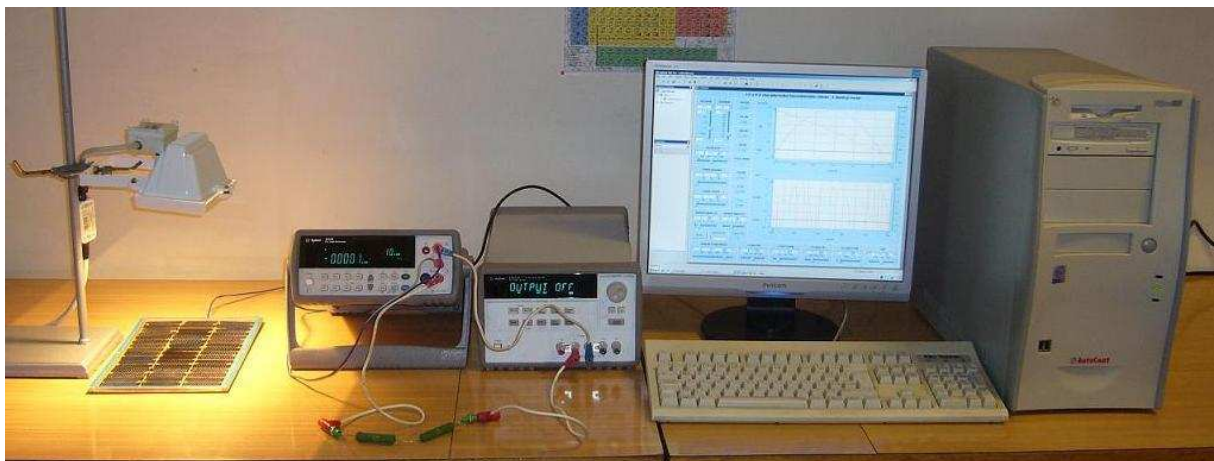


Fig. 7.3: Photo documentation involving wiring of laboratory instruments

7.1 Solar panel with circle cells

It is the solar panel created by series connection of 15 photovoltaic cells (see Fig. 7.4). These circular (or elliptical) cells are generated by cutting circle ingot. The cell is composed of polycrystalline silicon with a radius of $3 \cdot 10^{-2}$ m. Thus the area article is $2.82 \cdot 10^{-3}$ m². Individual cells are connected in the solar panel array at 3•5. The area of those 15 articles is $4.23 \cdot 10^{-2}$ m². The solar panel is encapsulated in the frame dimensions of $2.2 \cdot 10^{-1}$ m and $2.8 \cdot 10^{-1}$ m. Thus, the panel area is $6.16 \cdot 10^{-2}$ m².



Fig. 7.4: Solar panel with circle cells

For the solar panel measurements are carried out at two different distances from the lamp. The panel is illuminated by 150 W halogen lamp at a distance of $2 \cdot 10^{-1}$ m, where the measurement temperature is 328.15 K and the intensity of illumination is 368 W/m². The resulting characteristic is seen in Fig. 7.5 in case a) the distance is $2 \cdot 10^{-1}$ m. The same panel for further characterization, is measured by the same light at a distance of $4 \cdot 10^{-1}$ m, where the measurement temperature is 314.65 K and the irradiance is 124 W/m². The resulting characteristic is shown in Fig. 7.5, case b) distance of $4 \cdot 10^{-1}$ m.

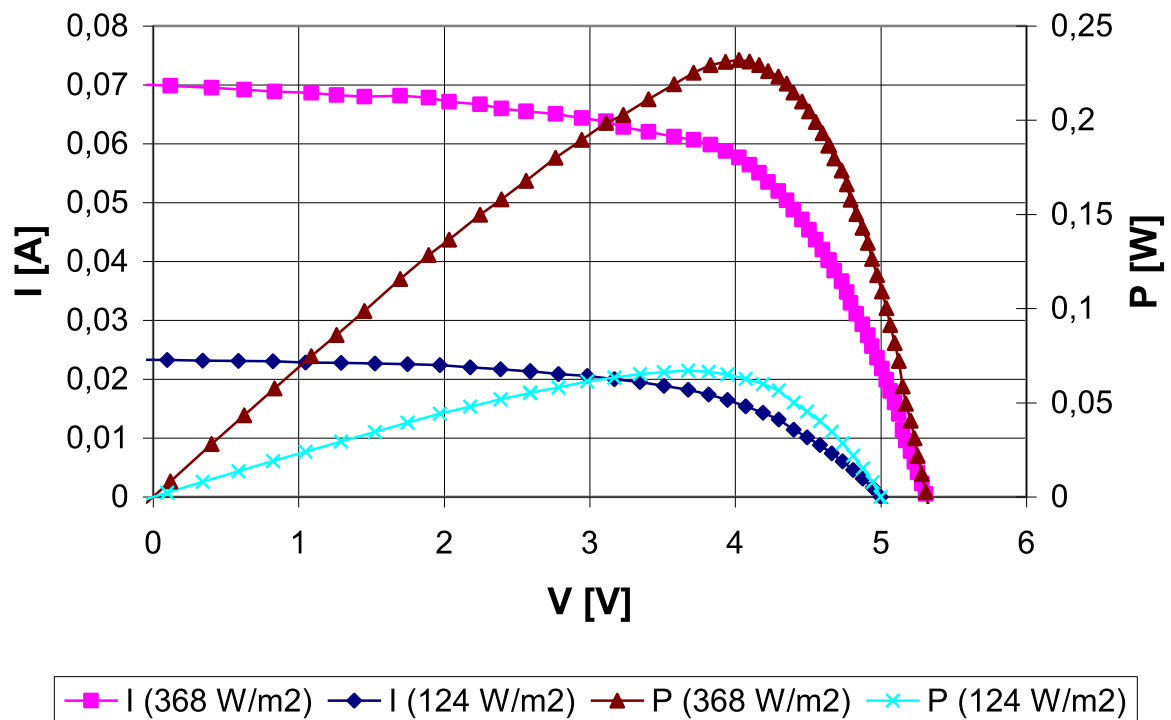


Fig. 7.5: I-V and P-V characteristics of the solar panel with circle cells in the light 150 W halogen lamp: a) distance of $h = 2 \cdot 10^{-1}$ m, $E = 368 \text{ W/m}^2$, other variables in Table 7.1; b) for distance $h = 4 \cdot 10^{-1}$ m, $E = 124 \text{ W/m}^2$, other variables in Table 7.2

Table 7.1: The characteristic data describing the real solar panel with circle cells in the intensity of irradiation 368 W/m^2

V_{OC}	I_{SC}	V_m	I_m	P_m	FF	η	T	A_{cell}	A_{panel}
[V]	[A]	[V]	[A]	[W]	[%]	[%]	[K]	[m ²]	[m ²]
5.381	$6.999 \cdot 10^{-2}$	4.025	$5.765 \cdot 10^{-2}$	$2.320 \cdot 10^{-1}$	61.61	1.491	328.0	$2.820 \cdot 10^{-3}$	$4.230 \cdot 10^{-2}$

Table 7.2: The characteristic data describing the real solar panel with circle cells in the intensity of irradiation 124 W/m^2

V_{OC}	I_{SC}	V_m	I_m	P_m	FF	η	T	A_{cell}	A_{panel}
[V]	[A]	[V]	[A]	[W]	[%]	[%]	[K]	[m ²]	[m ²]
4.999	$2.325 \cdot 10^{-2}$	3.677	$1.823 \cdot 10^{-2}$	$6.703 \cdot 10^{-2}$	57.68	1.278	315.0	$2.820 \cdot 10^{-3}$	$4.230 \cdot 10^{-2}$

7.2 Solar panel with rectangular cells

It is the solar panel created by series connection of 24 photovoltaic cells (see Fig. 7.6). The cell is composed of polycrystalline silicon with dimensions of $5.2 \cdot 10^{-2}$ m and $3.0 \cdot 10^{-2}$ m. Thus the area is $1.56 \cdot 10^{-3}$ m². Individual cells are connected in the solar panel array at 3•8. The area of all 24 cells is $3.744 \cdot 10^{-2}$ m². The solar panel is encapsulated in the frame dimensions of $1.8 \cdot 10^{-1}$ m and $2.7 \cdot 10^{-1}$ m. Thus the total area of the panel is $4.86 \cdot 10^{-2}$ m².



Fig. 7.6: Solar panel with rectangular cells

The panel is illuminated by 150 W halogen lamp at a distance of $2 \cdot 10^{-1}$ m, where the measurement temperature is 321.65 K and the intensity of illumination is 368 W/m². The resulting characteristic is in Fig. 7.7 a) distance of $2 \cdot 10^{-1}$ m. The same panel for further characterization, is measured by the light at the distance of $4 \cdot 10^{-1}$ m, where the measurement temperature is 306.65 K and the intensity of illumination is 124 W/m². The resulting characteristic is in Fig. 7.7 b) distance of $4 \cdot 10^{-1}$ m.

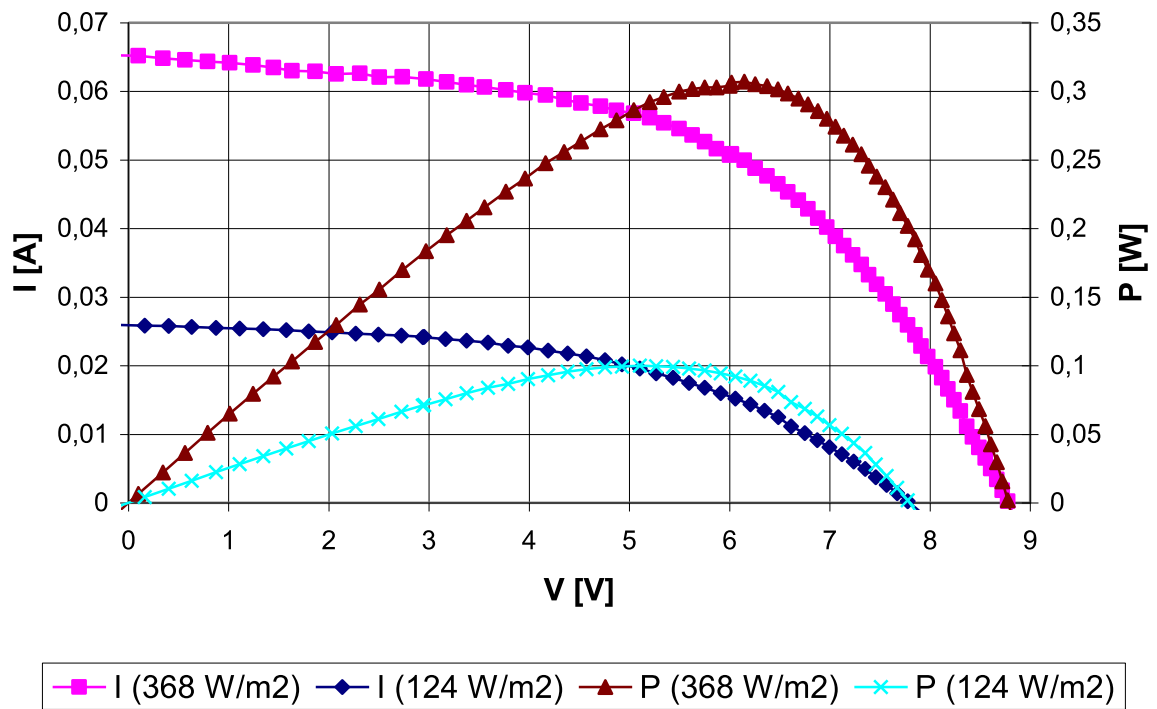


Fig. 7.7: I-V and P-V characteristics of the solar panel with rectangular cells in the light 150W halogen lamp) a) distance of $h = 2 \cdot 10^{-1}$ m, $E = 368$ W/m², other variables in Table 7.3 b) for distance $h = 4 \cdot 10^{-1}$ m, $E = 124$ W / m², other variables in Table 7.4.

Table 7.3: The characteristic data describing the real solar panel with rectangular cells in the intensity of irradiation 368 W/m²

V_{OC}	I_{SC}	V_m	I_m	P_m	FF	η	T	A_{cell}	A_{panel}
[V]	[A]	[V]	[A]	[W]	[%]	[%]	[K]	[m ²]	[m ²]
8.777	$6.520 \cdot 10^{-2}$	6.148	$4.996 \cdot 10^{-2}$	$3.072 \cdot 10^{-1}$	53.68	2.303	322.0	$1.560 \cdot 10^{-3}$	$3.744 \cdot 10^{-2}$

Table 7.4: The characteristic data describing the real solar panel with rectangular cells in the intensity of irradiation 124 W/m²

V_{OC}	I_{SC}	V_m	I_m	P_m	FF	η	T	A_{cell}	A_{panel}
[V]	[A]	[V]	[A]	[W]	[%]	[%]	[K]	[m ²]	[m ²]
7.777	$2.592 \cdot 10^{-2}$	4.024	$1.958 \cdot 10^{-2}$	$9.994 \cdot 10^{-2}$	49.57	2.195	307.0	$1.560 \cdot 10^{-3}$	$3.744 \cdot 10^{-2}$

8 SEARCHING CONSTANTS OF SOLAR PANEL

The procedure is that in real measurements, variables such as temperature, light intensity (irradiance), the area of panel, etc are known. Therefore, it is possible to portray I-V characteristic according to these values in our program (inducting the same values as in the real measurements). Our simulated I-V characteristic will vary over the measured I-V characteristic due to real different settings in the values of variables C_1 , C_2 , C_{S1} , R_S , R_P (applies to one-diode model). To achieve the same output for real time measurements of two-diode model it is necessary to set the values of variables C_{S1} , C_{S2} , C_1 , C_2 , R_S , R_P in our simulation programming model. Then the right setting constants can be achieved near-consensus, between the measured and simulated I-V characteristic of the solar panel.

Note: A complete identification between the measured and simulated I-V characteristic of the solar panel cannot be achieved, since in both cases of solar panels, solar cells are of different sizes, have different shapes, some cells in the panel are mechanically damaged, some series connections may be of poor quality. These panels are very outdated, as evidenced by the "bumpy" course of I-V characteristics, their effectiveness, the need to set up a big series resistance, etc. The comparison between simulated and measured I-V characteristics of the solar panel, therefore, can never, at least in this case be absolute consensus. However in the aspect of scholastic, these panels still serve their educational purposes.

Variables C_1 and C_2 are used to current settings. The correct setting is achieved by the exact value of short circuit current I_{SC} . Because the temperature and intensity of the real measurements, are known (see in recapitulation Table 8.1), from a distances of $2 \cdot 10^{-1}$ m and $4 \cdot 10^{-1}$ m, it is possible numerically to calculate the values of C_1 and C_2 of two equations with two unknowns. See in calculation C_1 and C_2 .

Table 8.1: The values needed to calculate the constants C_1 and C_2

	T	A ^{*1}	I _{SC} ^{*2}
	[K]	[$\cdot 10^{-2} \text{ m}^2$]	[$\cdot 10^{-2} \text{ A}$]
Solar panel with circle cells when $E = 124 \text{ W/m}^2$	314	0.282	2.325
Solar panel with circle cells when $E = 368 \text{ W/m}^2$	328	0.282	6.999
Solar panel with rectangle cells when $E = 124 \text{ W/m}^2$	307	0.156	2.593
Solar panel with rectangle cells when $E = 368 \text{ W/m}^2$	322	0.156	6.520

Note 1: Calculation I_{ph} is given for the cell of the area of $1 \cdot 10^{-2} \text{ m}^2$. In the case of the solar panel with circle cells area is $A_{\text{cell}} = 2.82 \cdot 10^{-3} \text{ m}^2$. In numerical computation, it is necessary to multiply the equation (16) by the appropriate coefficient of area A .

Note 2: In the zero voltage V there is a photo current I_{PH} equal to the short circuit current I_{SC} .

Calculation of C_1 and C_2 for the solar panel with circle cells:

$$I_{ph}(T) = (C_1 + C_2 T) E \cdot A$$

$$0,06999 = (C_1 + 328,15 \cdot C_2) \cdot 368 \cdot 0,282$$

$$0,023247 = (C_1 + 314,15 \cdot C_2) \cdot 124 \cdot 0,282$$

$$C_1 = \frac{67380557}{150129280000} = 4,49 \cdot 10^{-4} \frac{\text{m}^2}{V}$$

$$C_2 = \frac{5161}{7506464000} = 6,87 \cdot 10^{-7} \frac{\text{m}^2}{VK}$$

Calculation of C_1 and C_2 for solar panel with rectangular cells:

$$I_{ph}(T) = (C_1 + C_2 T) E \cdot A$$

$$0,0652 = (C_1 + 321,65 \cdot C_2) \cdot 368 \cdot 0,156$$

$$0,025927 = (C_1 + 306,15 \cdot C_2) \cdot 124 \cdot 0,156$$

$$C_1 = \frac{56702161}{10267200000} = 5,52 \cdot 10^{-3} \frac{\text{m}^2}{V}$$

$$C_2 = -\frac{91021}{6673680000} = -1,36 \cdot 10^{-5} \frac{\text{m}^2}{VK}$$

Changes in voltage V_{OC} can be achieved by setting the constant C_{S1} (in two-diode model is necessary also change constant C_{S2}). Another voltage change is possible through change of value of the diode factor. To simplify the counting of that the one ideal-diode

model is used, where the value of the diode factor is strictly set to 1. (In two ideal-diode factor the second diode factor is set to 2). This fact shows that change in the value of voltage V_{OC} is achieved only by the influence of constant C_{S1} , respectively constant C_{S2} in two-diode model. A parallel resistance R_P has a partial effect on the value of open circuit voltage V_{OC} .

Shape of I-V characteristic mediates the solar panel series resistance R_S and the parallel resistance R_P . With the increasing value of the series resistance R_S and the decreasing value of parallel resistance R_P , the I-V characteristics worsen, as it reduces FF, η (see in Fig. 8.1).

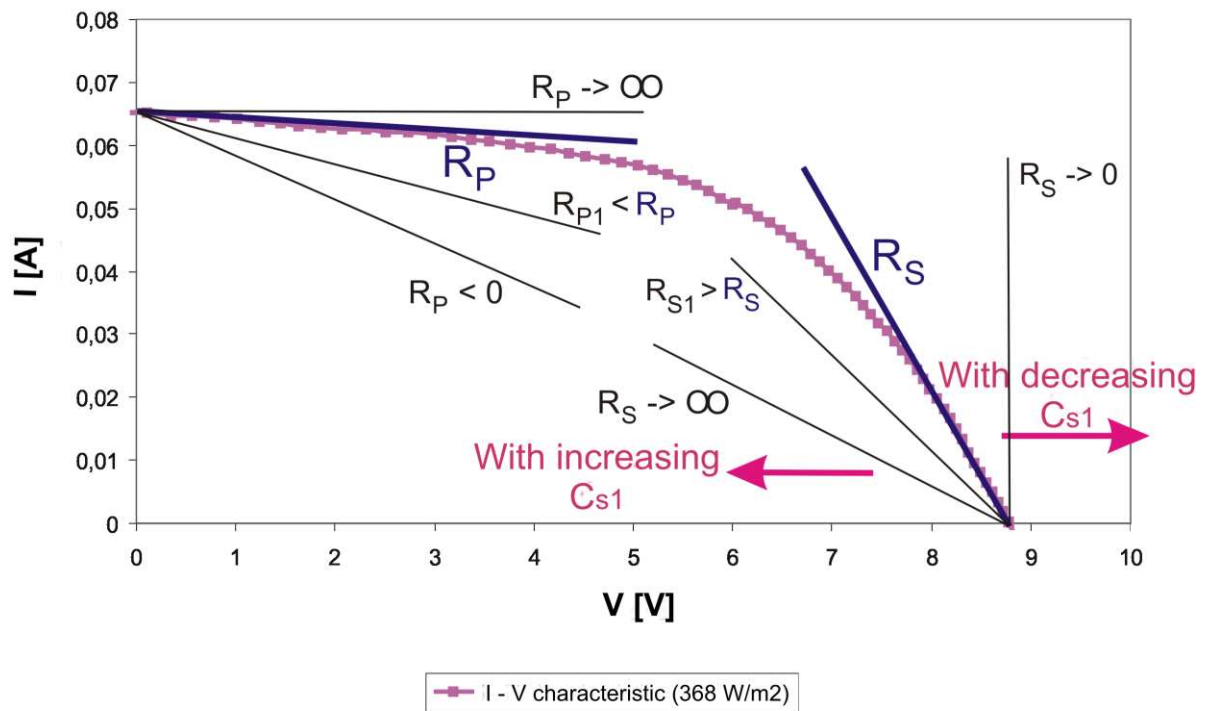


Fig. 8.1: Effect of setting the series and parallel resistance and constant C_{S1} to a final shape of I-V characteristics of the solar panel

Note: Curve in Fig. 8.1 is a real measured I-V characteristic of the solar panel with circle cells in the light intensity (irradiance) 368 W/m^2 and temperature 328 K . With the increasing value of constant C_{S1} , the curve shifts to the left. Value of the voltage V_{OC} decline. Decreasing the value of constant C_{S1} , makes the curve shift to the right and the open circuit voltage V_{OC} to increase.

8.1 Searched constants for solar panel with circle cells

In the case of the solar panel with circle cells, there were inducted values of constants C_1 , C_2 , C_{S1} , R_S and R_P like in Table 8.2. By comparing, using and trying between simulated and real I-V and P-V characteristic, the value of the constants has been obtained. Substituting these values into the simulation program using one-diode model (using interval methods), there can be compared variables such as V_{OC} , I_{SC} , etc. The values are in Table 8.3. Fig. 8.2 is a graphical comparison between simulated I-V and P-V characteristics of the solar panel with circle cells with characteristics of real and measured characteristics. Here it is seen that the curves are almost identical, which confirms the rightness of the substituted constant values. Absolute conformity of these curves cannot be achieved, since the cells are not dimensionally the same. It is possible to see more details in chapter SEARCHING CONSTANTS OF SOLAR PANEL.

Table 8.2: Values of constants that describe the most appropriate solar panel with circle cells

	R_S	R_P	C_1	C_2	C_{S1}
	[Ω]	[Ω]	[m^2/V]	[m^2/VK]	[A/K^3]
Real values					
Simulated values	$4.405 \cdot 10^{-1}$	43.91	$4.490 \cdot 10^{-4}$	$6.870 \cdot 10^{-7}$	782.2

Note: We do not know the values of the real constant of the real solar panel. Simulated values will be almost the same as the real values, because it is obtained almost the same I-V and P-V characteristic between simulated and real values. See in Table 8.3.

Table 8.3: Comparison of real measured with simulated values using one-diode model using interval method (measured in the solar panel with circle cells). Measured at irradiance 368 W/m^2

	V_{OC}	I_{SC}	V_m	I_m	P_m	FF	η
	[V]	[A]	[V]	[A]	[W]	[%]	[%]
Real values	5.381	$6.999 \cdot 10^{-2}$	4.024	$5.765 \cdot 10^{-2}$	$2.320 \cdot 10^{-1}$	61.60	1.490
Simulated values	5.379	$6.997 \cdot 10^{-2}$	3.980	$5.812 \cdot 10^{-2}$	$2.314 \cdot 10^{-1}$	61.47	1.486

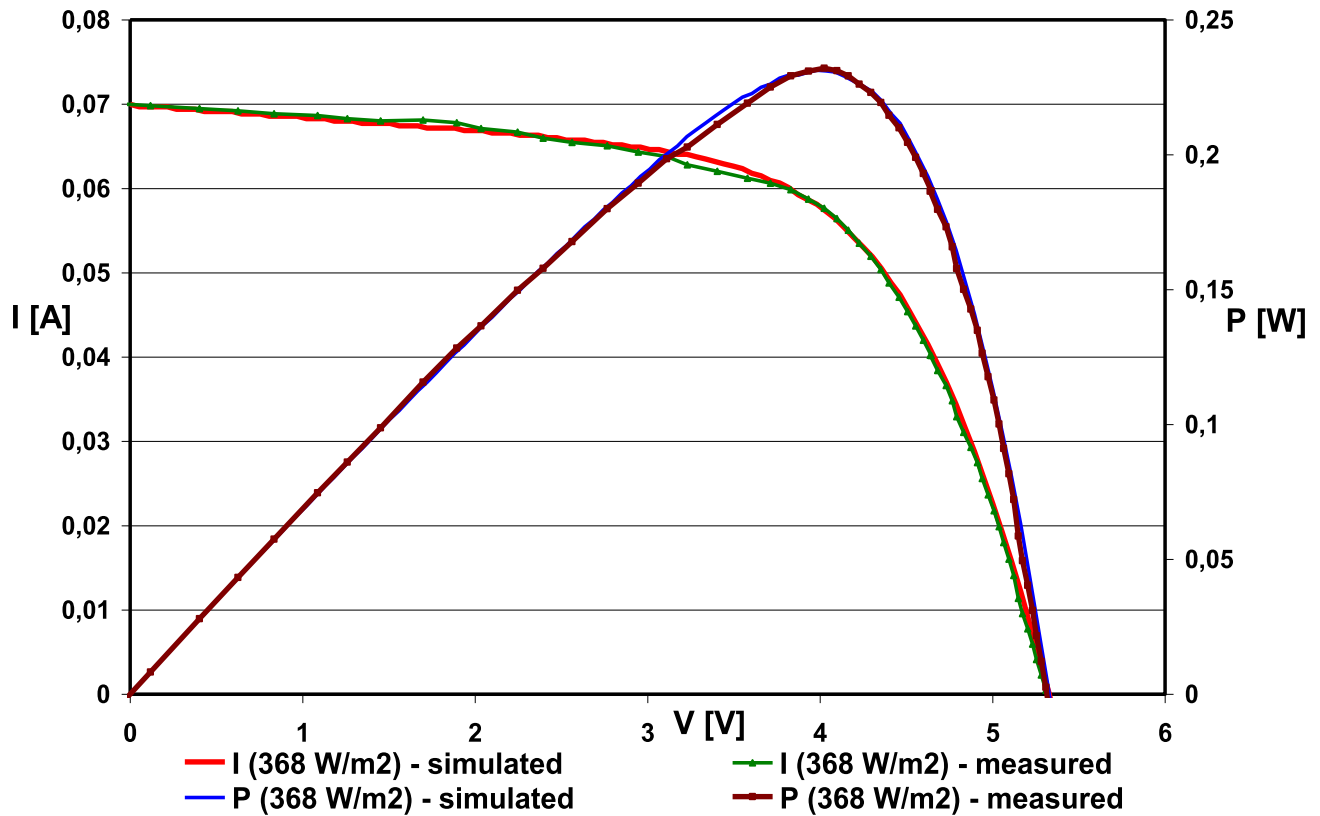


Fig. 8.2: I-V and P-V characteristic of solar panel with circle cells in the irradiance 368 W/m² when setting values of constants C_1 , C_2 , C_{S1} , R_S , R_P like in the Table 8.2

8.2 Searched constants for solar panel with rectangular cells

In the case of the solar panel with rectangular cells, values of constants C_1 , C_2 , C_{S1} , R_S and R_P were inducted values like in Table 8.4. By comparing, using and trying between simulated and real I-V and P-V characteristic, the value of the constants has been obtained. Substituting these values into the simulation program using one-diode model (using interval methods), there can be compared variables such as V_{OC} , I_{SC} , etc. The values are in Table 8.5. Fig. 8.3 is a graphical comparison between simulated I-V and P-V characteristics of the solar panel with round cells with characteristics of real and measured characteristics. Here it is seen that the curves are almost identical, which confirms the rightness of substituted constant values. Absolute conformity of these curves cannot be achieved, since the cells are not dimensionally the same. More details can be seen in chapter SEARCHING CONSTANTS OF SOLAR PANEL.

Table 8.4: Values of constants that describe the most appropriate solar panel with rectangular cells

	R_S	R_P	C_1	C_2	C_{S1}
	[%]	[%]	[m ² /V]	[m ² /VK]	[A/K ³]
Real values					
Simulated values	2.865	53.44	$5.520 \cdot 10^{-3}$	$-1.360 \cdot 10^{-5}$	8364

Note: We do not know the values of the real constant of the real solar panel. Simulated values will be almost the same as the real values, because it is obtained almost the same I-V and P-V characteristic between simulated and real values. See in Table 8.5.

Table 8.5: Comparison of real measured with simulated values using one-diode model using interval method (measured in the solar panel with rectangular cells). Measured at irradiance 124 W/m²

	V_{OC}	I_{SC}	V_m	I_m	P_m	FF	η
	[V]	[A]	[V]	[A]	[W]	[%]	[%]
Real values	7.777	$2.593 \cdot 10^{-2}$	5.103	$1.958 \cdot 10^{-2}$	$9.999 \cdot 10^{-2}$	49.56	2.195
Simulated values	7.874	$2.590 \cdot 10^{-2}$	5.090	$1.978 \cdot 10^{-2}$	$1.007 \cdot 10^{-2}$	49.37	2.114

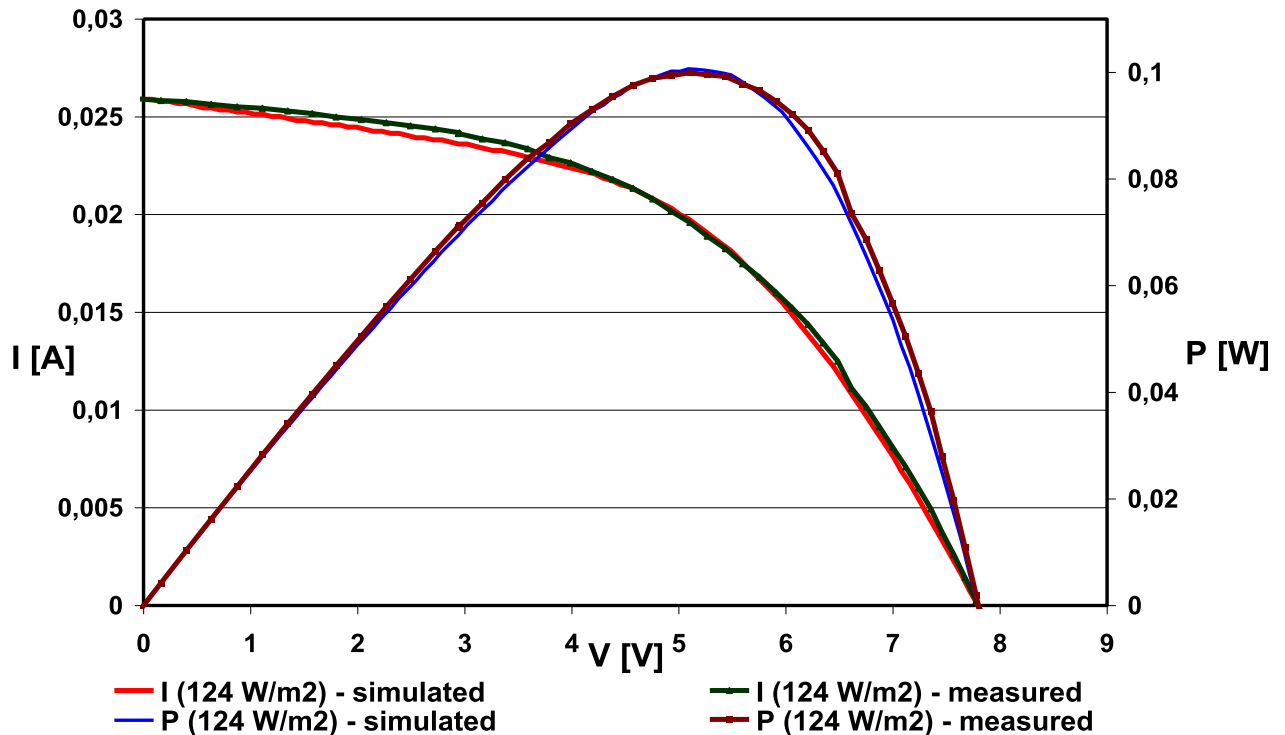


Fig. 8.3: I-V and P-V characteristic of solar panel with rectangular cells in the irradiance 124 W/m² when setting values of constants C_1 , C_2 , C_{S1} , R_S , R_P like in the Table 8.4

9 CONCLUSION AND OUTLOOK

In the program VEE Pro 8.0 was simulated the program that plots the I-V and P-V characteristics of the solar panel. First the incremental method has been used. This, however, when entering extreme input variables failed. Thus, there has been developed a new method for simulating, called the interval method, which bypasses the problem and accurately plots the I-V and P-V characteristics of solar panel even in extreme input parameters.

The program is very extensive. In the simulation, software can be set too many different variables such as the influence of temperature, light intensity, series resistance, parallel resistance, area of cell, diode factor. Furthermore, you can set the number of series connected cells and the number of parallel connected cells, but only if the cells are the same. In the screen you can clearly see the necessary information, such as open circuit voltage V_{OC} , Short circuit current I_{SC} , voltage V_{MPP} , current I_{MPP} , number of used cells, power of system P_{MPP} , Fill-factor FF, and the efficiency η of panel. For user convenience, in the program there is an important button Excel. Push the button Excel to export all necessary data in a table in Microsoft Excel. It also generates useful charts of I-V and P-V characteristics of solar cell, or panel (with series, parallel, series or parallel configuration) and the second graph, which describes the values of calculated currents for each step.

As well, there was also built a fully automated workplace, where real measurements on real panels were performed. For each solar panel there were simulated two I-V and P-V characteristics and always at different intensities of light. Correspondence between measured and simulated I-V and P-V characteristics has been nearly reached, which gave us the so necessary values of the constants describing the solar panel.

Based on this program can be continued the simulation of shaded solar cells, various wiring, bypass diodes, series, parallel or series-parallel connection nonconforming cells, etc.

This program is not just for testing solar panels, identifying their essential characteristics, but also because of its versatility it can be used for teaching students. There is already a laboratory exercise for students built on this work. This exercise is about dependency of the irradiance and temperature on the I-V characteristic. Its potential is to teach students quite a lot in the area of photovoltaic.

LIST OF FIGURES

Fig. 2.1: Solar panel	7
Fig. 3.1: Bend model.....	8
Fig. 3.2: Crystal Structure of Silicon (left), intrinsic conduction due to	9
Fig. 3.3: Defect Conduction for n-type (left) and p-type doped silicon (right)	10
Fig. 3.4: Model of electrons and holes of intrinsic semiconductor	12
Fig. 3.5: Model of P-N junction	14
Fig. 3.6: Cut commonly produced typical solar cells.....	15
Fig. 4.1: The production P-N junction of solar cells	17
Fig. 4.2: The production of contacts by screen-printing	18
Fig. 4.3: Polycrystalline, square solar cell.....	18
Fig. 5.1: Dependence of band gap width on temperature.....	19
Fig. 5.2: Extended equivalent circuit of a solar cell (one-diode model).....	21
Fig. 5.3: Influence of the series resistance R_S to I-V characteristics of solar cell	22
Fig. 5.4: Influence of the parallel resistance R_P to I-V characteristics of solar cell	22
Fig. 5.5: Extended equivalent circuit of a solar cell (two-diode model)	23
Fig. 5.6: I-V and P-V characteristics of solar cell with maximum power point P_{MPP}	25
Fig. 5.7: I-V characteristics of the temperature dependence on solar cells	28
Fig. 5.8: Series connection of photovoltaic solar cells	29
Fig. 5.9: I-V of the solar panels up to 36 potential cells in the series connection	30
Fig. 5.10: Parallel connection of n photovoltaic solar cells	30
Fig. 6.1: Block diagram of the incremental method.....	33
Fig. 6.2: Operational screen of one-diode model for the program using incremental method	34
Fig. 6.3: Block diagram of interval method	35
Fig. 6.4: Operational screen of one-diode model for the program using interval method.....	36
Fig. 6.5: I-V characteristic of one-diode model of the solar panel at random constants (see Table 6.1).....	38
Fig. 6.6: The values of currents at various iterations (one-diode model).....	38
Fig. 6.7: I-V characteristics of two-diode model of solar panel at random values of constants (see Table 6.1) ...	39
Fig. 6.8: The values of currents at various iterations (two-diode model).....	40
Fig. 6.9: Scheme of measurement irradiance in different distances of source of light.....	41
Fig. 6.10: Dependence of light intensity of 150 W halogen lamp on distance from pyranometer	41
Fig. 6.11: Temperature dependence on time in light 150W halogen lamp at a distance of $1 \cdot 10^{-1}$ m, $2 \cdot 10^{-1}$ m, $4 \cdot 10^{-1}$ m (862 W/m^2 , 368 W/m^2 , 124 W/m^2).....	42
Fig. 7.1: Schematic wiring circuit for the measuring of I-V characteristic of the solar panel.....	43
Fig. 7.2: Alternative wiring circuit for measuring I-V characteristic of a solar panel (including computer)	44
Fig. 7.3: Photo documentation involving wiring of laboratory instruments.....	44
Fig. 7.4: Solar panel with circle cells	45
Fig. 7.5: I-V and P-V characteristics of the solar panel with circle cells in the light 150 W halogen lamp: a) distance of $h = 2 \cdot 10^{-1}$ m, $E = 368 \text{ W/m}^2$, other variables in Table 7.1; b) for distance $h = 4 \cdot 10^{-1}$ m, $E = 124 \text{ W/m}^2$, other variables in Table 7.2	46
Fig. 7.6: Solar panel with rectangular cells	47
Fig. 7.7: I-V and P-V characteristics of the solar panel with rectangular cells in the light 150W halogen lamp) a) distance of $h = 2 \cdot 10^{-1}$ m, $E = 368 \text{ W/m}^2$, other variables in Table 7.3 b) for distance $h = 4 \cdot 10^{-1}$ m, $E = 124 \text{ W/m}^2$, other variables in Table 7.4.	48
Fig. 8.1: Effect of setting the series and parallel resistance and constant C_{S1} to a final shape of I-V characteristics of the solar panel	51
Fig. 8.2: I-V and P-V characteristic of solar panel with circle cells in the irradiance 368 W/m^2 when setting values of constants C_1 , C_2 , C_{S1} , R_S , R_P like in the Table 8.2.....	53
Fig. 8.3: I-V and P-V characteristic of solar panel with rectangular cells in the irradiance 124 W/m^2 when setting values of constants C_1 , C_2 , C_{S1} , R_S , R_P like in the Table 8.4.....	54

REFERENCES

University mimeographed:

[1] VANĚK, J.; KŘIVÍK, P.; NOVÁK, V. *Alternativní zdroje energie*. ELEKTRONICKÉ SKRIPTUM VUT Brno 2006

Periodical:

[2] LIBRA, M., POULEK, V.. SVĚTLO 2005/1, Fyzikální podstata fotovoltické přeměny energie [online]. 2005 [cit. 2008-05-30], pp. 32-36. Available in the WWW:
<http://www.odbornecasopisy.cz/download/sv010532.pdf>

Internet:

[3] *Sluneční energie* [cit. 2010-02-05]. Available in the WWW:
http://cs.wikipedia.org/wiki/Sluneční_energie

[4] Zemánek R., Principle of the photovoltaic, PN junction. 2008-2009 Available in the WWW:
<http://fotovoltika.falconis.cz/fotovoltika/prechod-pn.php>

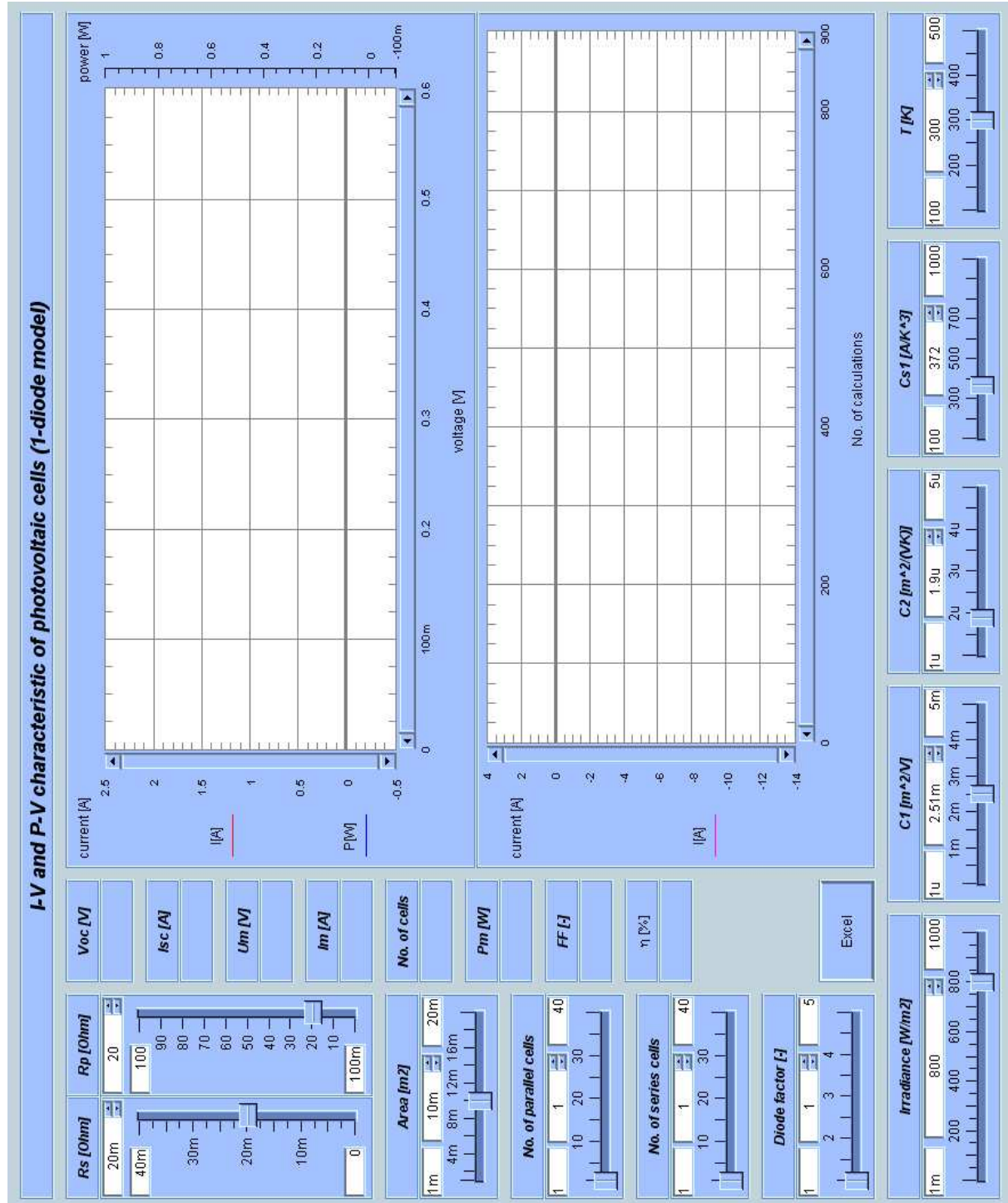
Books:

[5] B. Van Zeghbroeck, Semiconductor Fundamentals, 2.3.3.3 Temperature dependence of the energy bandgap 2007. Available in the WWW:

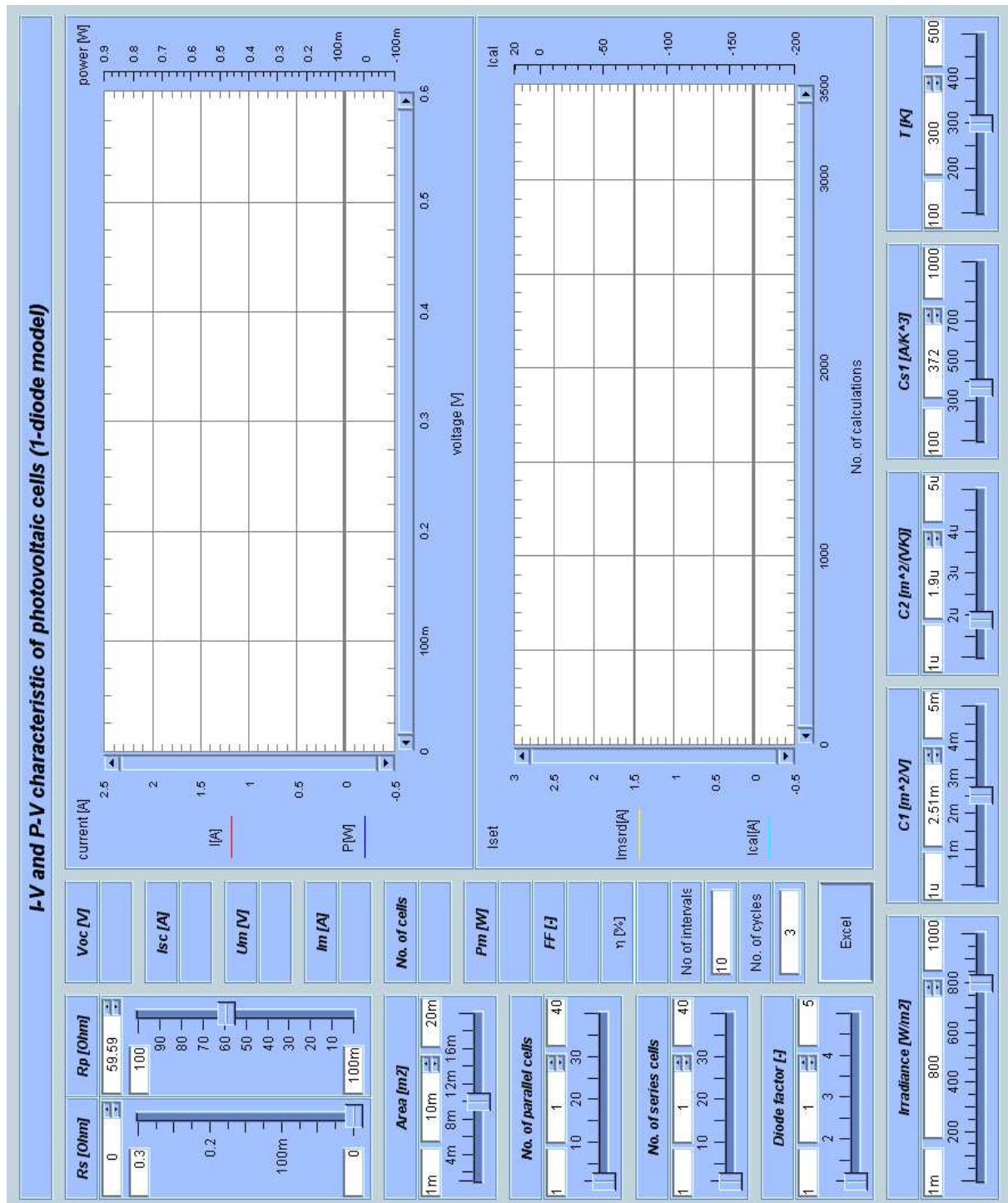
<http://ecee.colorado.edu/~bart/book/book/chapter2/ch2_3.htm#tab2_3_2>

[6] QUASCHNING, V., *Understanding renewable energy systems* USA 2007, p. 118-148;
ISBN 978-1-84407-136-4

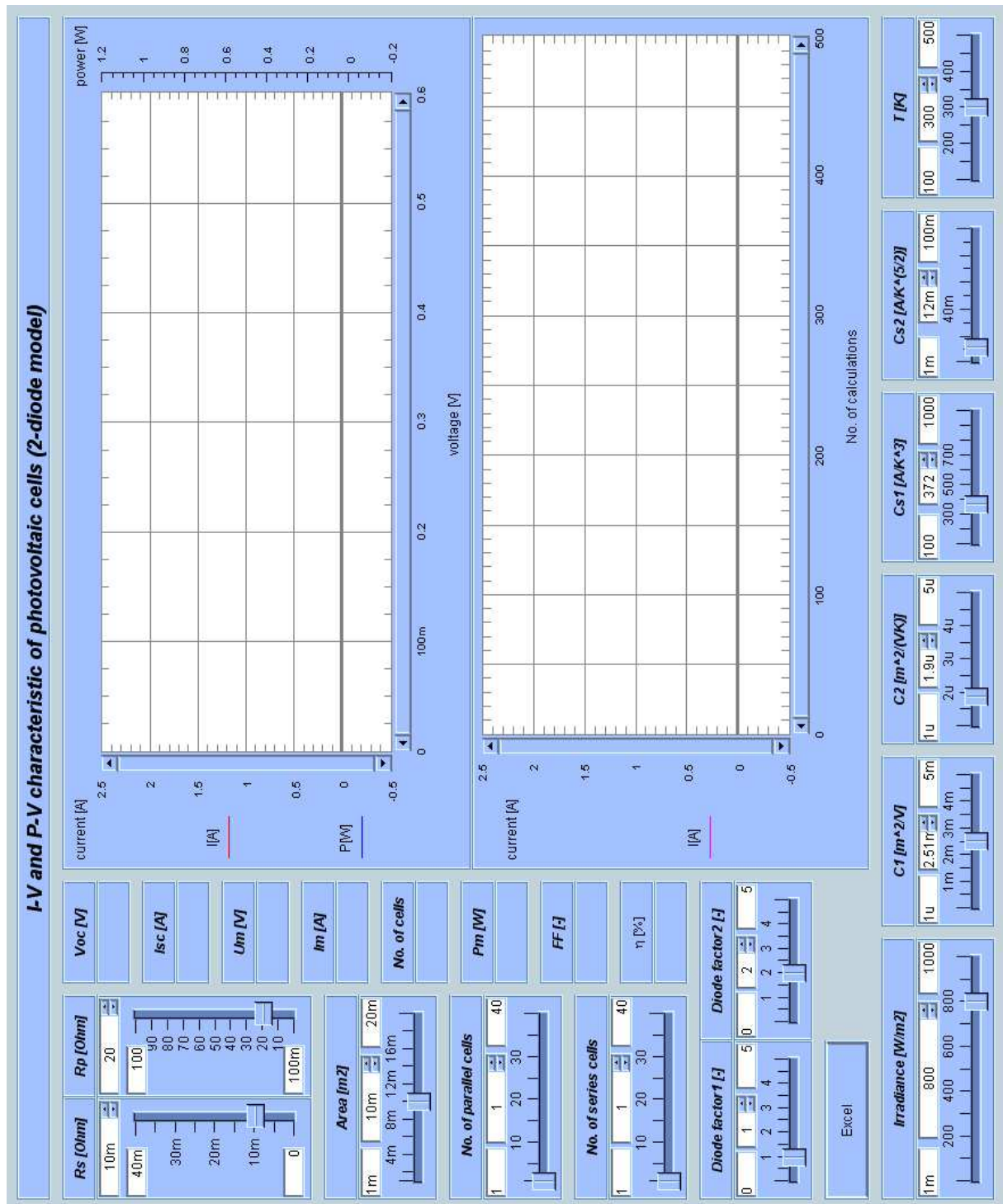
ANNEXES



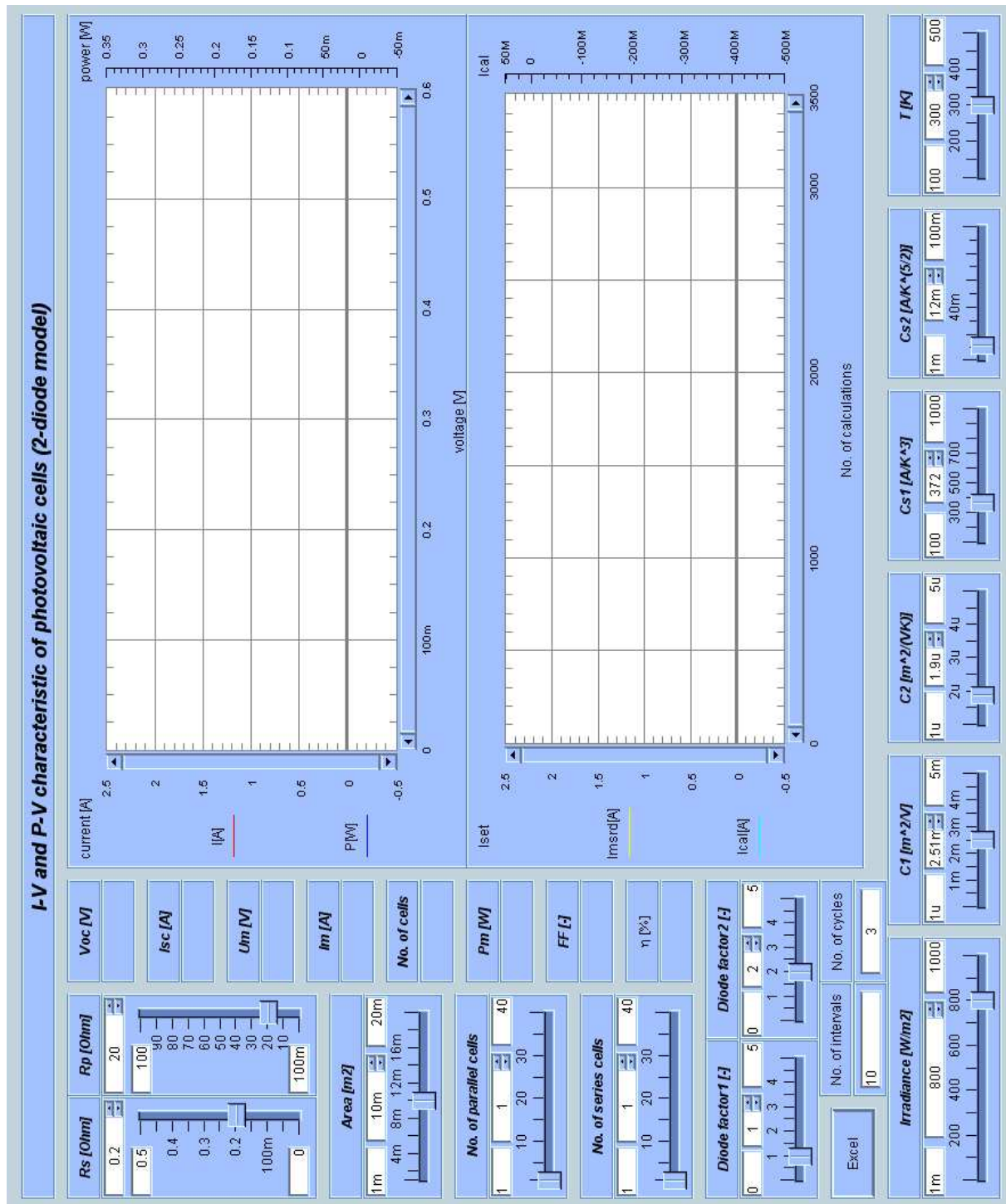
Appendix A: Operational screen of one-diode model for the program using incremental method




Appendix B: Operational screen of one-diode model for the program using interval method



Appendix C: Operational screen of two-diode model using incremental method



Appendix D: Operational screen of two-diode model using the interval method

measuring interval [s]		measuring cycle	
<input type="text" value="60"/>		<input type="text" value="0"/>	
number of cycles	temperature [°C]		
<input type="text" value="1500"/>	<input type="text"/>		
			

Appendix E: Operational screen of program for measuring the temperature